5-2014

No-Independent Modulation Of Soluble Guanylyl Cyclase (Sgc) Activity And Function

George L. Britton Jr

NO-INDEPENDENT MODULATION OF SOLUBLE GUANYLYL CYCLASE (sGC) ACTIVITY AND FUNCTION

By

George L. Britton

APPROVED:

_____

Emil Martin, PhD
Supervisory Professor

_____

Eric Wagner, PhD

_____

Richard Kulmacz, PhD

_____

Jeff Frost, PhD

_____

Phillip Carpenter, PhD

APPROVED:

_____

Dean, The University of Texas
Graduate School of Biomedical Sciences at Houston

NO-INDEPENDENT MODULATION OF SOLUBLE GUANYLYL CYCLASE (sGC) ACTIVITY AND FUNCTION

A
Thesis

Presented to the Faculty of

The University of Texas

Health Science Center at Houston

And

The University of Texas

MD Anderson Cancer Center

Graduate School of Biomedical Sciences

In Partial Fulfillment

of the Requirements

for the Degree of

MASTER OF SCIENCE

by

George L. Britton, B.S.

Houston, Texas

May 2014

Nitric Oxide (NO)-Independent Modulation of Soluble Guanylyl Cyclase (sGC) Activity and Function

George L. Britton, M.S.

Advisory Professor: Emil Martin, Ph.D.

Soluble guanylyl cyclase (sGC) plays a key role in the nitric oxide (NO) signaling pathway, where it functions as an NO receptor and generator of a secondary intracellular messenger, cGMP. In addition to NO, investigators have identified a number of proteins that interact with sGC and modulate its function. For example, the interaction of sGC with ADP-ribosylation factor GTPase activating protein 1 (AGAP1) governs sGC's intracellular distribution and therefore mediates localized production of cGMP. Interactions of sGC with heat-shock protein 90 (HSP90) or HSP70 promote the extent of sGC activation upon NO stimulation, while interaction of sGC with the η subunit of chaperonin-containing T-complex polypeptide 1 (CCTη) or with protein disulfide isomerase (PDI) decreases NO-stimulated cGMP production. Previous experiments demonstrated that the G-protein signaling modulator protein, activator of G-protein signaling 3 (AGS3), attenuates the response of sGC to activators in cell lysates.

In this report, we provide evidence that sGC activity and responsiveness are increased in AGS3-deficient mice. We found that AGS3-deficient mice not only have a lower resting blood pressure than their wild-type counterparts, but also are more sensitive to sGC agonists (DEA-NO and BAY41-2272). Hematoxylin and eosin staining of aorta sections did not show any significant no

morphological differences between AGS3$^{-/-}$ and wild type mice. However, sGC in aortic lysates from AGS3$^{-/-}$ mice generated a higher level of cGMP in response to the NO-donor, DEA-NO, than in wild type lysates. These data indicate that, in the absence of AGS3, sGC activity is increased within smooth muscle cells of aortic tissue. In summary, the data from the present study suggests that AGS3 is a negative regulator of sGC vascular function.

TABLE OF CONTENTS

ILLUSTRATIONS

TABLES

ABBREVIATIONS

AGS : Activator of G-protein signaling
Arnt: Aryl hydrocarbon receptor
bp: base pair
H&E : Hemtoxylin and Eosin
AC : Adenylyl Cyclase
AGAP1 : ADP-ribosylation factor GTPase activating protein 1
AGS3 : Activator of G-protein signaling 3
AGS3-/- : Activator of G-protein signaling 3 knockout mice
BAY41-2272 : 3-(4-Amino-5-cyclopropylpyrimidine-2-yl)-1-(2-fluorobenzyl)-1H-pyrazolo[3,4-b]pyridine
Ca^{2+} : Calcium ion
CaM : Ca^{2+}/Calmodulin
cAMP : Adenosine monophosphate
CCTη : Chaperonin containing t-complex polypeptide subunit η
cGMP : Cyclic guanosine monophosphate
CNG : Cyclic-nucleotide gated
DEA-NO : diethylamine NONOate
DTT : Dithioreitol
EM : Electron microscopy
eNOS : endothelial nitric oxide synthase
GDI : Guanine nucleotide dissociation inhibitor
GDP : Guanosine diphosphate
GEF : Guanine nucleotide exchange factor
GPR : G-protein regulatory motif
GTP : Guanine-5'-triphosphate
HDX-MS: Hydrogen/deutrium exchange mass spectrometry
His105 : Histidine 105
H-NOX : N-terminal Heme-Nitric Oxide/Oxygen
HSP70 : Heat-shock protein 70
HSP90 : Heat-shock protein 90
IBMX : 3-isobutyl-1-methylxanthine
IP : Intraperitoneal
IP3 : Inosital triphosphate
LGN : Leu-Gly-Asn enriched protein
MABP : Mean Arterial Blood Pressure
MCLP : Myosin light-chain phosphatase
MLCK : Myosin light-chain kinase
NO : Nitric Oxide
NOS : nitric oxide synthase

OC: Occlusion Cuff
OCT : Optimal Cutting Temperature
PAS : Per-Arnt-Sim
PBS : Phosphate buffered saline
PDE : Phosphodiesterase
PDI : Protein disulfide isomerase
Per : Period circadian protein
PKG : cGMP-dependent protein kinase
qRT-PCR : Quantative reverse transcriptase polymerase chain reaction
SERCA : Sarco/endoplasmic reticulum Ca^{2+} - ATPase
sGC : Soluble Guanylyl Cyclase
Sim : Single minded protein
SNP : Sodium nitroprusside
SR : Sarcoplasmic reticulum
TLC : Thin Layer Chromatography
TPR : Tetratricopeptide repeats
VPR : Volume Pressure Recording
Wild type mice: C57BL/6
WT : Wild Type

INTRODUCTION

1. NO-cGMP Signaling:

In eukaryotic cells, nitric oxide (NO) is a critical diatomic signaling molecule influencing various physiological processes such as smooth muscle relaxation, neurotransmission, and platelet aggregation (1-3). Soluble guanylyl cyclase (sGC) is the primary intracellular receptor for NO-signaling. NO activates, by several hundred fold, the sGC-mediated conversion of guanine-5'-triphosphate (GTP) into the intracellular secondary messenger cyclic guanosine monophosphate (cGMP) (Fig. 1). Once formed, the second messenger, cGMP, is responsible for targeting phosphodiesterases (PDE), cyclic-nucleotide gated (CNG) channels and cGMP-dependent protein kinases (PKG) (4).

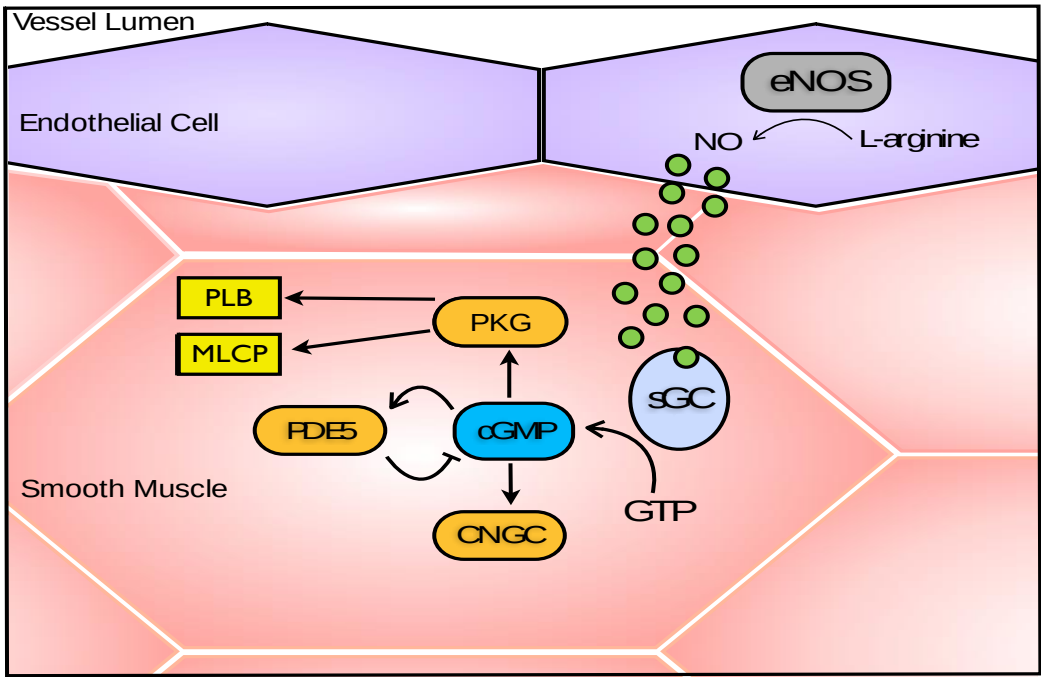

Figure 1. The NO/sGC/cGMP signaling pathway in blood vessels. eNOS catalyzes the production of NO by conversion of L-arginine to L-citrulline (L-Cit) and NO. NO diffuses into the smooth muscle cells where it binds to the heme moiety of sGC, activating the enzyme and increasing cGMP levels. cGMP subsequently binds to and activates PKG, PDEs, and CNG channels. PKG can promote smooth muscle cell relaxation by its interaction with many of its downstream effectors, such as phospholamban (PLB) and myosin light-chain phosphatase (MLCP).

This report is centered on understanding an alternative method in regulating sGC function, with primary focus on sGC function in vascular smooth muscle cells. Therefore, the function of the NO-sGC-cGMP signaling transduction pathway will be mainly discussed within the context of smooth muscle cells of the cardiovascular system.

NOS - In mammalian cells, NO is synthesized by a family of nitric oxide synthases (NOS). Three isoforms of NOS are known, with different tissue

Table 1. Tissue specific expression of various NOS isoforms.

Name	Location	Function
Neuronal Nitric Oxide Synthase (nNOS)	skeletal muscle nervous tissue	cell communication
Inducible Nitric Oxide Synthase (iNOS)	immune system	immune defense
Endothelial Nitric Oxide Synthase (eNOS)	vascular endothelium	vasodilation

distribution (Table 1) (5). In the cardiovascular system, endothelial NOS (eNOS) is the main source of NO production and resides in the endothelial layer of the vasculature (6). Shear forces on the endothelial membrane and/or hormonal signals binding to endothelial surface receptors cause a surge in intracellular Ca^{2+} levels and induce the formation of the Ca^{2+}/Calmodulin complex (7). This complex leads to subsequent calmodulin (CaM)-dependent activation of eNOS (8). Thereafter, eNOS catalyzes the oxidation of the amino acid L-arginine to produce both NO and L-citrulline (9). After its production, NO diffuses across the endothelial membrane into vascular smooth muscle cells, where it can bind with

sGC to transmit the NO signal to its various downstream cGMP-dependent effectors, PKG, PDE, CNG channels (9).

PDE – cGMP is hydrolyzed to GMP by a family of phosphodiesterases, an enzyme that breaks the phosphodiester bonds of cyclic nucleotides (10). Collectively, eleven different PDE families and their various splice variants share common cellular functions: to regulate the duration, localization and magnitude of cyclic nucleotide signaling (11). The diversity in PDE functions stem from differences in their structures, cellular localization, expression profiles, kinetic properties, and inhibitor sensitivities (11). Each PDE isoform demonstrates distinctive substrate selectivity. For example, PDE5, 6 and 9 are cGMP-selective, while PDE4, 7 and 8 are cAMP-selective (12). Some PDEs are capable of hydrolyzing both cAMP and cGMP (PDE1, 2, 3, 10, and 11) (12). PDE inhibitors are commonly used to maintain intracellular level of cGMP. For example, sildenafil, a PDE5 inhibitor, is often used as a tool that allows investigators to quantitate sGC activity from the accumulation of cGMP in response to NO (13).

PKG - The steady state levels of cGMP in the cells as determined by the relative rates of cGMP formation by guanylyl cyclases and its degradation by PDE ultimately controls the activation of PKG (4) (Fig. 2). Activated PKG promotes relaxation of smooth muscle cells. This is achieved through direct phosphorylation of myosin light-chain phosphatase (MLCP) (14), and the control of intracellular Ca^{2+} levels (15). PKG-dependent phosphorylation of MLCP activates its phosphatase function, which subsequently inhibits smooth muscle contraction by dephosphorylating myosin light-chain fibers that were

phosphorylated by myosin light kinase (MLCK). In doing so, the phosphatase activity of MLCP disrupts the cross-bridge between actin and myosin in the contracted state, and thus promotes smooth muscle cell relaxation (14). Second, PKG acts to inhibit smooth muscle contraction by keeping intracellular Ca^{2+} below the levels that signal the cell to contract (16). This latter effect is

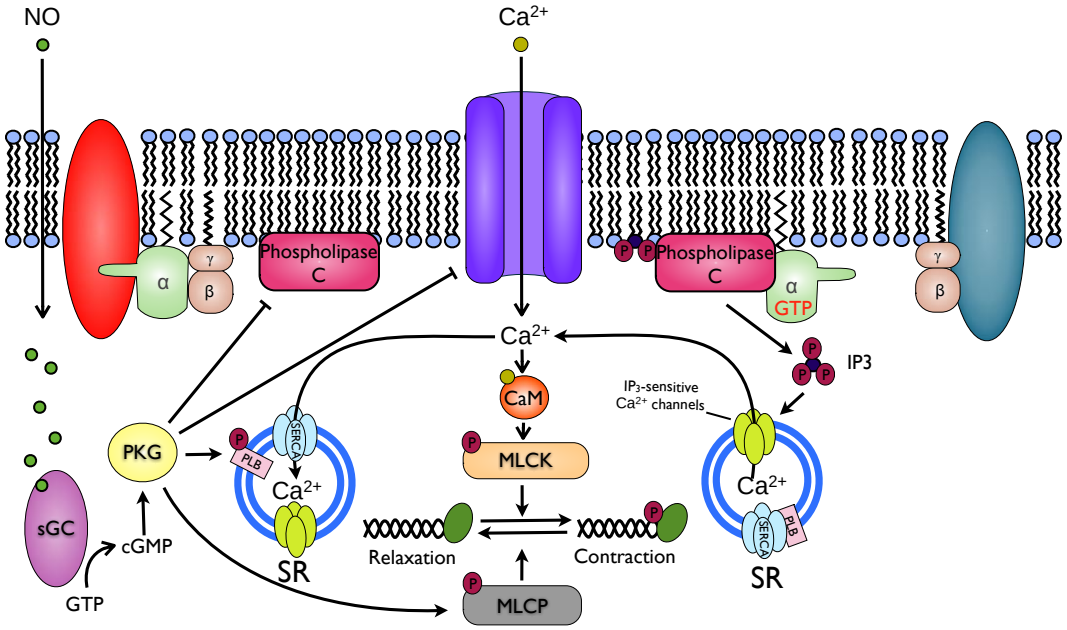

Figure 2. Possible molecular signaling pathways associated with PKG mediated smooth muscle cell relaxation. Upon elevated levels of intracellular Ca^{2+} derived from the sarcoplasmic reticulum (SR) or the extracellular space, Ca^{2+}/calmodulin (CaM) complex is formed, which results in the activation of MLCK. MLCK phosphorylates the myosin light chain fibers signaling the cell to form cross bridges between actin and myosin. PKG reverses the contracted state of smooth muscle cells by: 1) activating MLCP; and 2) decreasing intracellular Ca^{2+} levels due to sequestration of Ca^{2+} through SERCA channels located in the SR, and inhibiting L-type Ca^{2+} channels, and preventing formation of IP_3 by inhibiting phospholipase C.

accomplished by PKG through several possible mechanisms. These include phosphorylation of phospholipase C, resulting in reduced generation of inositol triphosphate (IP_3), and phosphorylation of the negative regulatory phospholamban protein. Phospholamban is associated with the

sarco/endoplasmic reticulum Ca^{2+}-ATPase (SERCA), and phospholamban phosphorylation increases the activity of SERCA (15). The overall result of PKG activity is the decreased availability of intracellular Ca^{2+} levels in smooth muscle cells. This restricts the CaM-dependent activation of the myosin-actin cross bridging enzyme MLCK.

CNG Channels - cGMP is also known to bind to and activate CNG channels (15). Initially discovered as part of the phototransduction pathway for retinal photoreceptors, CNG channels also act as nonselective cation channels to mediate the entry of extracellular Ca^{2+} into vascular smooth muscle cells (17).

2. Soluble Guanylyl Cyclase

Because sGC lies at the nexus between the beneficial effects of NO-signaling and cGMP-dependent downstream targets, it is an interesting therapeutic target. Before the function of sGC and its therapeutic potential were discovered, organic nitrates were commonly used by physicians to treat patients with angina and heart failure (18,19). It wasn't until the 1980s that researchers determined the connection between sGC activation by endogenous NO and cardiovascular events. To better understand the processes that control and modulate sGC function, an understanding of sGC structure-function relationships is needed.

2.1 sGC isoforms and structure

Mammalian sGC consists of one α subunit (73 kDa, 690 aa) and one β subunit (70 kDa, 619 aa). Two isoforms (α1/α2 and β1/β2) encoded by separate genes (GUCY1A2, GUCY1A3, GUCY1B2 and GUCY1B3) exist for each sGC

subunit (20). The α1/β1 heterodimer is the main and ubiquitously expressed sGC variant, while the α2/β1 heterodimer is expressed primarily in neurons (21). Pharmacological and biochemical kinetic studies conducted by Russwurm et al. (22) demonstrated that the naturally occurring sGC isoforms, α1/β1 and α2/β1, exhibit similar sensitivities to NO despite differences in the primary structure of the α1 and α2 subunits. Further studies (23) show that the differential biological effects of the isoforms are based on their localization: α2/β1 has a propensity to localize at the membrane, whereas the α1/β1 sGC is primarily localized in the cytosol.

As demonstrated in Figure 3, each sGC subunit is composed of four domains: an N-terminal Heme-Nitric Oxide/Oxygen (H-NOX) domain, a (Per-ARNT-Sim) PAS domain, a coiled-coil domain, and a C-terminal catalytic domain (9).

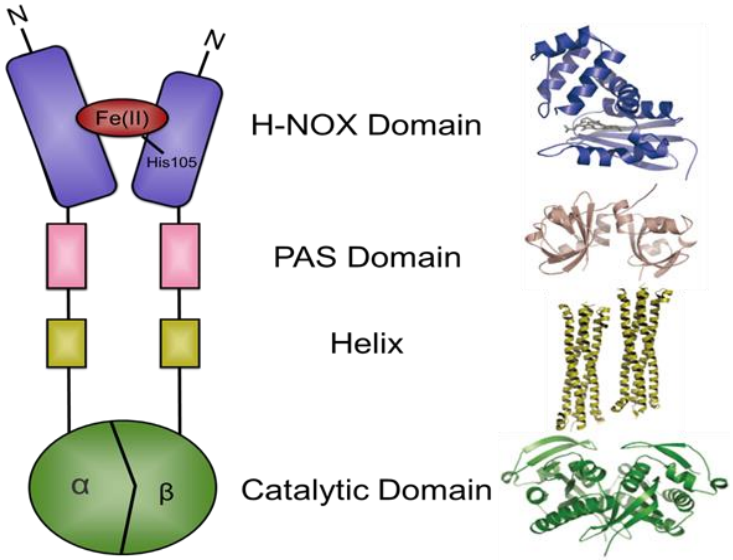

Figure 3. Structural organization of sGC functional domains. Schematic representation of sGC domain organization is shown on the left. Known x-ray structures are shown on the right. Crystal structures of H-NOX, PAS, coiled-coil and catalytic domains were adapted from Ref [9] with permission from Annual Review of Biochemistry.

2.1.1 H-NOX domain

The N-terminal region of sGC is a critical structure that harbors the heme prosthetic group and provides sGC the ability to sense NO, and to transduce the message to the catalytic domain. Using a series of α1 N-terminal truncation mutants of sGC, investigators determined that the NO-sensing heme prosthetic group resides in the β subunit of the protein (24). For example, spectral, biochemical, and pharmacological analyses showed that the first 259 amino acids of the H-NOX domain in α1 could be deleted and still preserve an NO-sensitive sGC complex (24). Further spectral and kinetic studies characterized N-terminal fractions of the β1 subunit (25). A fragment containing residues 1-385 of β1 was found to contain stoichiometric amounts of heme (25). This β1(1-385) fragment had the same characteristic UV-spectrum and spectral shifts after NO addition as the full-length heterodimeric sGC (25), indicating that the N-terminus of β1 is the primary heme-containing domain of sGC. Site-directed mutagenesis demonstrated that His105 of the β1 subunit coordinates the heme moiety (26). Subsequent experiments determined that the His105 mutation does not directly affect heterodimerization of sGC subunits or the function of the catalytic domain (26). Any substitution of β1His105 abolished heme binding and the capacity of sGC to respond to NO stimulation (26).

2.1.2 PAS domain

The PAS domain is named after the three proteins in which it was initially discovered: 1) Per-period circadian protein; 2) Arnt-aryl hydrocarbon receptor nuclear translocator protein; and 3) Sim-single-minded protein (27). Despite

differences in their amino acid sequences, PAS domains share a conserved three-dimensional architecture that functions as a signal sensor (27). In sGC, the PAS domain appears to perform similarly. Results from a recent study using hydrogen/deuterium exchange mass spectrometry (HDX-MS) suggested that the PAS domain of sGC communicates the proximate NO-induced conformational changes in the H-NOX domain to the catalytic domain (28). HDX-MS analysis identified NO-dependent perturbations not only within the PAS domain, but also at the intersection between the PAS and coiled-coil domains (28). Importantly, these perturbations extend through to the highly flexible coiled-domain domain and ultimately influence the catalytic domain to reconfigure into an active state (28).

2.1.3 Coiled-coil Domain

The coiled-coil domain in sGC appears to be unique in that it forms an S-helical structure and, to date, shares little homology with other proteins deposited in the National Center for Biotechnology Information protein database (29). The crystal structure of the coiled-coil domain was characterized for the β1 subunit (residues 348-409) and discovered to form tetrameric arrangements of coiled-coil dimers. The coiled-coils are likely arranged in parallel, which allows the flanking sGC domains to align correctly (29). In comparison, anti-parallel coiled-coil arrangements were shown to form stable, but non-functional, β1 homodimeric sGC (29). This is likely the result of the improper alignment of the flanking domains, which prevents the formation of a catalytically active enzyme. Additional studies have suggested that amino acids Leu394 and Pro399 play

significant roles in the dimerization and activation of sGC (29).

2.1.4 Catalytic Domain

The catalytic domains of sGC isoforms are not only highly homologous to one another, but also share a high degree of homology with particulate guanylyl cyclase and adenylyl cyclase (AC) (15). Therefore, a considerable amount of knowledge in the function of the catalytic domain of sGC first emerged through homology modeling with the crystal structure of AC. Investigators found that the residues used in substrate recognition and catalysis for AC were located on the cytoplasmic C1 and C2 domains (30). The corresponding domains were attributed to α1 and β1 of sGC (31). The use of heterologous expression systems has allowed investigators to confirm these assignments *in vitro*. For instance, transient expression of either α1 or β1 subunits alone in COS-7 cells yielded no sGC activity, whereas co-expression of both subunits produced fully functional sGC that was responsive to sodium nitroprusside (SNP), an NO-releasing compound (32). These data indicate that although each subunit contains a catalytic domain, both α1 and β1 are required to form an active catalytic site.

2.1.5 sGC Architecture

To date, full-length heterodimeric sGC has proven to be resistant to crystallization, which hampers our understanding of its mechanism of action. Studies aimed at elucidating the detailed molecular structure of full-length sGC have had to resort to crystallizing homologous proteins from bacteria, algae, or work with separate isolated domains. None of these approaches allow investigators to gain understanding of the structure-function relationship between

sGC domains. Recent developments in the use of high-throughput single-particle electron microscopy (EM) has, however, provided a three-dimensional model of a heterodimeric sGC holoenzyme architecture (33). This approach has provided some understanding of the higher-order domain architecture of sGC and its various configurations (33) (Fig. 4A,B). Additionally, it has allowed Campbell et

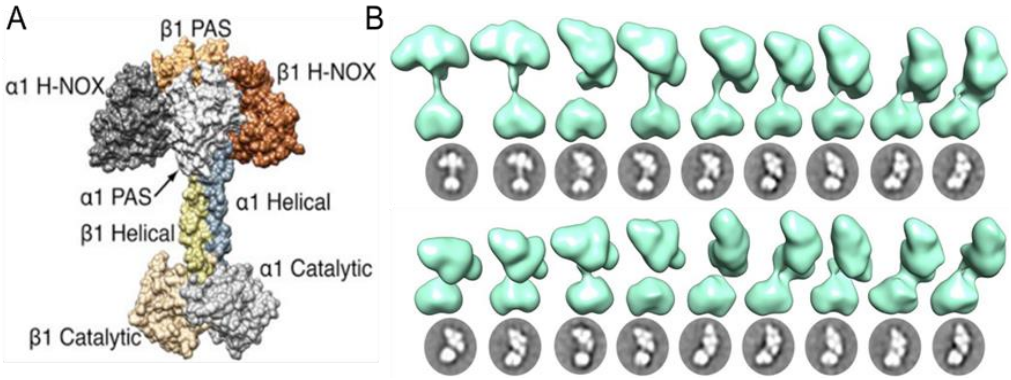

Figure 4. The flexible coiled-coil domain lends to a unique structure and function of sGC. **(A)** The higher-order domain architecture of sGC organized into 2 modular domains with the coiled-coil linking the two halves together. **(B)** Range of conformations observed in sGC holoenzyme. 3-dimensional reconstructions are shown in green, while 2-dimensional images are down below. Model of sGC and its conformational snapshots were reprinted with permission from Proceedings of the National Academy of Sciences, Single-Particle EM Reveals the Higher-Order Domain Architecture of Soluble Guanylate Cyclase, Campbell et al., 2014. Vol. 111 no. 8: 2960-5.

al. (33) to characterize the function of the highly-flexible coiled-coil domain of sGC. The results showed that the coiled-coil domain is configured in a dimeric parallel coiled-coil that flexibly bridges two modular ends of sGC. One end includes the catalytic domain, while the second half consists of a complex formed between the PAS and H-NOX domains. It appears, that the coiled-coil allows the two modular ends to freely swing over a continuous range of conformations (Fig. 4B). The degree of flexibility in sGC is demonstrated by the ability of the H-NOX domain at the N-terminus to contact the C-terminal catalytic domain (33). This

characteristic flexibility may play an important role in allowing sGC to rapidly and accurately respond to various cellular signals that modulate its activity.

2.2 sGC Activation

In the basal state, sGC has a relatively low turnover rate of 15-20 min^{-1}(9). However, upon NO binding to the heme moiety, the enzymatic activity is increased by ~100-fold to a turnover rate of more than 1800 min^{-1} (9). Details of the activation mechanism are currently under investigation. It is well accepted that NO binds to the heme of sGC to form an unstable 6-coordinate complex, which rapidly converts into a 5-coordinate complex due to the disruption of the coordinating bond between His105 and the heme iron (9) (Fig. 5). sGC

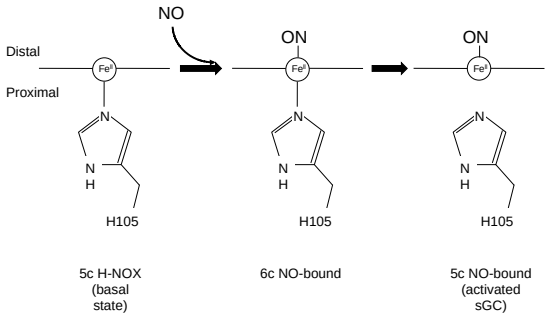

Figure 5. Hypothetical mechanism of sGC activation. Binding of NO to sGC heme produces a transient 6-coordinate complex, followed by disruption of the coordinating bond between β1 His105 and the heme iron. This results in formation of the 5-coordinate nitrosyl-heme and activation of sGC.

containing this 5-coordinate NO-heme complex has a high cGMP-forming activity. Once NO dissociates from sGC, the production of cGMP falls back to the basal rate (9). This indicates that sGC activity can be quickly up- and down-regulated to ensure proper functioning of NO-dependent signaling processes (9). It also suggests that the NO-sGC interaction or the subsequent conformational changes leading to sGC activation may be the subject of regulation by various exogenous factors.

3. Exogenous factors affect sGC function:

While NO is the well-established ligand and activator of sGC, a growing body of evidence suggests that other cellular factors also influence the extent or the duration of sGC activation. For example, sGC activation by NO is stronger in the native cellular environment than *in vitro*, and exhibits a difference in activity depending on the cells in which sGC is expressed (34). In other studies, it was demonstrated that the rate of cGMP synthesis is significantly increased in response to NO stimulus only for a brief period of time. This stimulated state of intracellular sGC is followed by a quick desensitization, which is not explained by enhanced PDE activity or decomposition of NO (35). The authors suggested that intact cells may contain factors that lead to rapid desensitization of sGC.

Investigators have begun to identify several proteins that bind sGC and modulate its function. Binding of sGC with (1) ADP-ribosylation factor GTPase activating protein 1 (AGAP1) governs sGC intracellular distribution and therefore localizes production of cGMP (36); (2) heat-shock protein 90 (HSP90) and HSP70 increase NO-stimulated sGC activation (37,38); and (3) chaperonin-containing T-complex polypeptide 1, η subunit (CCTη) and protein disulfide isomerase (PDI) each impede NO-stimulated cGMP production (39,40).

4. LGN and AGS3:

This list of possible sGC interactors and modulators has recently been updated to include LGN, a protein identified for its 10 leucine-glycine-asparagine repeats, and its close homolog activator of G-protein signaling 3 (AGS3) (41). LGN and AGS3 are members of a family of proteins known as receptor-

independent activators of G-protein signaling (AGS) (42). Initially discovered in a yeast-based functional screen as a factor involved in promoting G-protein signaling independent of a G-protein coupled receptor, AGS proteins are now known to influence the processing of cellular signals by acting as alternative binding partners for G-protein subunits (42). Over the past decade, a confluence of biochemical data has put various AGS proteins into three groups, based upon the mechanism of interaction with G-proteins (43). Group 1 AGS proteins function as guanine nucleotide exchange factors (GEF) and therefore increase G-protein signaling turnover rates (43). Group 2 AGS proteins act as guanine nucleotide dissociation inhibitors (GDI) and impede $G\alpha_i$-protein signaling (43). Group 3 AGS proteins interact with $G_{\beta\gamma}$, but their functions are not yet well understood (43). Both LGN and AGS3 belong to group 2 of AGS proteins (43). These proteins have a 3-module domain organization and share 59% amino acid sequence homology. As shown in Figure 6, the N-terminal domain containing seven tetratricopeptide repeats (TPR) is separated by a linker region from a C-terminal GoLoco domain that contains four G-protein regulatory (GPR) motifs (41,44). Recent evidence indicates that each GPR motif binds and stabilizes one $G_{\alpha i}$ in the GDP-bound conformation. It has been suggested that AGS3 and LGN

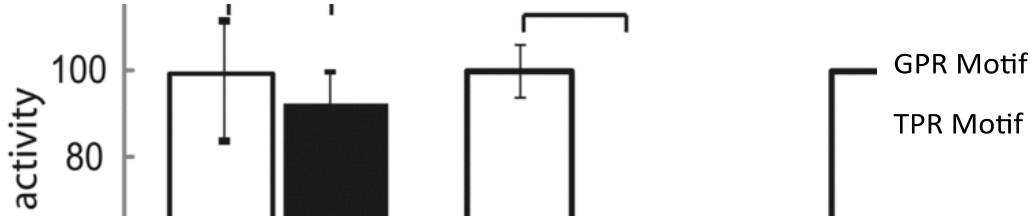

Figure 6. Similar organization of AGS3 and LGN proteins. Both LGN and AGS3 have 7 tetratricopeptide repeats (TPR) at their N-terminal domain, and 4 G-protein regulatory (GPR) motifs at their C-terminal GoLoco domain.

may serve as scaffolding proteins within a larger signaling complex (42,45). These discoveries have broadened the perspectives on the role of G-protein signaling.

It is now understood that LGN directly interacts with sGC (46). Yeast two-hybrid screens against α1 or β1 sGC as baits identified LGN as a possible sGC interactor (46). The sGC-LGN complex was co-precipitated from cultured cells and tissue homogenates. A series of co-immunoprecipitation studies using purified full-length and truncated isoforms of LGN and sGC indicate that the TPR domain of LGN and the catalytic domain of sGC are required for the interaction (46). The effects of this interaction were later examined in experiments monitoring the activity of sGC when LGN is either overexpressed or knocked-down. The results showed that LGN overexpression resulted in lower sGC activity in cellular lysates, whereas knockdown of LGN transcription mediated higher sGC activity (46). Collectively, these *in vitro* data suggest that LGN is a negative modulator of both the basal and activated states of sGC (46). The homologous AGS3 protein was also shown to inhibit sGC, but with more effect on activated sGC. In other studies performed by Blumer et al (47), mice lacking AGS3 had a NO-dependent drop in mean arterial blood pressure that was considerably longer than in wild-type counterparts. These studies suggest that AGS3 may function as a possible component in the molecular processes that alter sGC activity in the NO/cGMP signaling pathway

AIMS

The main goal of my study was to investigate how AGS3 affects sGC function. I hypothesized that, similar to LGN, AGS3 acts as a negative modulator of sGC, and that AGS3 deficiency should result in increased sGC activity in vivo. To test this hypothesis, I pursued the following specific aims:

1) Determine the effect of AGS3-deficiency on sGC-mediated regulation of blood pressure; and

(2) Determine the effect of AGS3-deficiency on sGC activity in tissue extracts.

METHODS:

Mice:

All animal manipulations were approved by the Animal Welfare Committee at the University of Texas Health Science Center at Houston. C57BL/6 wild type mice were purchased from Harlan Laboratories, Inc. AGS3 null mice were obtained from the laboratory of Dr. Stephen Lanier at the Medical University of South Carolina. Wild type and AGS3-null mice were housed in separate cages at the University of Texas Health Science Center's Animal Core Facility in a controlled environment: 12-h light/12-h dark cycle; 22°C; and free access to water and food. Body weight (25-28 grams) for each mouse was assessed prior to blood pressure measurements.

Genomic DNA Isolation:

Genomic DNA was extracted and isolated from ear samples of $AGS3^{-/-}$ and wild type mice using a DNeasy kit (Qiagen). Tissue samples were transferred quickly to a microcentrifuge tube containing a premixed solution of 180 µl of "ATL" Buffer (proprietary) and 20 µl of proteinase K provided by Qiagen, mixed thoroughly by vortexing for 20 seconds, and subsequently incubated at 56°C overnight to ensure complete tissue lysis. The next day, each tube was vortexed for 15 seconds and 200 µl of "AL" buffer added. Again, samples were vortexed for 15 seconds, before adding 200 µl of ethanol to each tube. Genomic DNA was isolated using Qiagen filter columns following the company protocol. Each wash was removed by centrifugation at 6000 x g for 1 minute. DNA was then eluted with 50 µl of sterile water.

Amplification of Genomic DNA by PCR:

Genomic PCR was used to detect the deletion of exon 3 in the AGS3 gene of AGS3$^{-/-}$ mice. The following primers were used for this purpose: forward (5'-TCA GAG CCA TCC TGA CTG CAT AGA-3') and reverse (5'-TGA TTG CAG GAG CTG TGT TCT AGT-3'). 250 ng of genomic DNA was mixed with a master mix containing: 2.5 µl of 10x Taq Buffer (Fisher), 2 µl of 2.5 mM dNTP mix, 2 µl of 10 µM forward primer, 2 µl of 10 µM reverse primer, 0.25 µl of Taq polymerase (5000 units/ mL) (Fisher), 12.75 µl of water, and 1.5 µl of 2 mM $MgCl_2$. PCR was performed using the following cycling conditions: 94ºC, 120 seconds; followed by 35 cycles of 94ºC for 30 seconds, 60ºC for 60 seconds and 72ºC for 45 seconds. Following PCR, samples were analyzed by electrophoresis in a 3% agarose gel.

Mean Arterial Blood Pressure Measurements:

The CODA tail-cuff system (Kent Scientific, Boston MA) was used in all blood pressure recordings. This system uses Volume Pressure Recording (VPR) to non-invasively measure changes in blood pressure. Wild type and AGS3 -/- mice were acclimated to the experimental conditions and equipment for 3 days prior to recording data. Each mouse was comfortably restrained in the provided animal holder, and safely positioned on a warming plate for at least 15 minutes to maintain a body temperature of 32- 35°C. During this time, the occlusion cuff (OC) and VPR cuffs were threaded together at the base of the tail and secured in a comfortable position to minimize discomfort for the mouse. Mean arterial blood pressure (MABP) was determined from the CODA-designed VPR and occlusion cuff by measuring the total blood volume in each tail from conscience mice. At

the conclusion of each experiment, mice were immediately removed from the holder and returned to their cages. Blood pressure recordings were acquired by a central CODA controller and data collector for further analysis.

Resting Mean Arterial Blood Pressure Measurements:

Resting MABP was evaluated in AGS3 -/- and wild type (n=8) preconditioned mice using the CODA tail-cuff system as described above. Both animal groups experienced 10 acclimation cycles prior to recording the MABP. Blood pressure measurements were recorded at 36-second intervals over 36 minutes.

Effects of sGC Activator Administration on MABP:

To evaluate the effects sGC agonist have on vasomotor control in AGS3 -/- (n=16) and wild type (n=10) animals, mice were randomly divided into two treatment groups: (1) one intraperitoneal (IP) injection of a NO-donor, 2-(N,N-diethylamino)diazenolate-2-oxide, diethylammonium salt (DEA-NO; 80 µg/kg; Cayman Chemical); or (2) one IP injection of an NO-independent sGC allosteric activator (BAY41-2272; 200 µg/kg; Cayman Chemical). MABP was recorded in both treatment groups in preconditioned mice using the CODA tail-cuff system. Baseline blood pressure changes following IP injection of sterile PBS (200 µl) were recorded for 20 minutes prior to the injection of sGC agonist. Injections were made through a hole drilled in the animal holder. Following the IP injections of agonists, blood pressure was recorded at 36-second intervals over a period of 20 minutes.

Tissue Homogenate Preparation:

The descending aorta from wild type or AGS3 -/- mice was surgically removed, homogenized in a glass-glass conical tissue grinder and sonicated in an ice bath for 16 seconds total with 4-second pulses. To separate residual tissue debris from cellular lysate homogenates were centrifuged at 5,000 x g for 15 minutes at 4 °C. Supernatants were subsequently centrifuged at 100,000 x g for 1 hour at 4°C to separate the membrane fraction (pellet) from the cytosolic fraction. Each fraction was placed into a separate microcentrifuge tubes and stored at -80 °C for later use. Sample protein amounts were determined by the implementation of a Bradford assay. Absorbance values from a dilution-series of unknown samples are interpolated onto a plot for the standard (bovine serum albumin) to determine sample protein concentrations.

Phosphodiesterase Activity:

To measure total tissue PDE activity, [α-^{32}P] GTP was first converted to [α-^{32}P] cGMP by reacting with purified sGC at 37 °C in reaction buffer (4 mM $MgCl_2$, 0.05 mg/ml creatine kinase, 5 mM phosphocreatine,125 mM triethanol amine (TEA), and 1 mM dithiothreitol (DTT)). Reactions were stopped by briefly heating the samples at 100 °C. The reaction product, [α-^{32}P] cGMP, was used as substrate to measure PDE activity in mice aortic lysates with or without a nonspecific PDE inhibitor, IBMX (1 mM) or a PDE5 specific inhibitor, Sildenafil (200 μM). All reactions were incubated in a 37 °C water bath for 15 minutes and heat inactivated at 100°C for 3 minutes. Samples were then centrifuged for 5 minutes at room temperature to pellet the precipitated proteins. An aliquot of

each supernatant (10 µl) was then analyzed by thin layer chromatography (TLC) on a pre-washed polyethyleneimine cellulose plate in a solvent system containing equal volumes of 0.5 M of ammonium acetate (pH 6) and 0.5M of ammonium formate (pH 4). [α-^{32}P] GTP alone with reaction buffer, or in the presence with purified sGC were used as controls to determine cGMP and GTP migration position The bands corresponding to substrate and product were visualized by X-ray film autoradiography overnight at -80 °C, and quantified by densitometric analysis using NIH ImageJ software.

sGC Activity Assay:

Soluble guanylyl cyclase activity in aortic lysates was assayed in the presence or absence of 100 µM NO donor DEA-NO by the formation of [α-^{32}P] cGMP from [α-^{32}P] GTP. Following tissue lysate separation by centrifugation, 20 µl of aortic tissue supernatants were mixed with 10 µl of reaction buffer (125 mM TEA, 250 µM EGTA, 10 mM IBMX, 4 mM MgCl2, 0.05 mg/mL creatine kinase, 5 mM creatine phosphate, 1 mM DTT, 100 µM GTP, 500 µM GTP/0.08 µCi of [α-^{32}P] GTP). After incubating at 37°C for 10 minutes, reactions were stopped by heat-inactivation for 3 minutes at 100°C. Reaction products were separated and quantified by TLC, as described above.

Western Blots:

Tissue lysate proteins were separated by SDS/polyacrylamide gel electrophoresis (8% gels) and transferred to PVDF membranes. Membranes were blocked with 5% milk containing 0.1% Tween-20 for 30 minutes and incubated with the desired primary antibody for 2 hours at room temperature or

overnight at 4 °C. Primary antibodies were: anti-α1 polyclonal antibodies (Sigma Aldrich, catalog # G4280) (1:1000 dilution); anti-LGN goat polyclonal antibody (AbCam, catalog # ab84571) (1:1000 dilution); and anti-α-actin polyclonal antibody (Sigma Aldrich, catalog # SAB2500963) (1:2000 dilution). For detection of β1, polyclonal antibodies raised in rabbits against the SRKNTGTEETKQDDD peptide of human sGC β1- subunit conjugated to KHL were used (1:500 dilution). Membranes were then washed three times for 10 minutes with 1X Tris Buffered Saline with Tween-20 (TBS-T). The horseradish peroxidase-conjugated secondary antibodies were used at dilutions of 1:3000 (anti-mouse, Sigma catalog # MFCD00162644) or 1:5000 (anti-rabbit, catalog # MFCD00162788; and anti-goat, catalog # MFCD00162340) dilutions. Membranes were then washed three times with TBS-T for 10 minutes. Immunoreactive bands were visualized on Kodak Biomax X-ray film by enhanced chemiluminescence (ECL Plus, GE Healthcare). Densitometric analysis was performed using NIH ImageJ. Probed proteins were normalized to either α-actin from smooth muscle cell samples, or β-actin from lung samples.

Histology/Autofluorescence:

Descending aortas from AGS3 -/- and wild type mice were quickly removed following cervical dislocation, embedded in optimal cutting temperature compound (OCT) by flash freezing in liquid nitrogen and stored at -80°C. Frozen samples were serially cut into 5 μm sections using a Microm 505E cryostat and transferred to microscope slides. Each specimen was dehydrated in 95% ethyl alcohol solution for 30 seconds, briefly rehydrated by submerging in water for 10

seconds and then stained with Shandon Gill 3 Hematoxylin (Thermo Scientific) for 4 minutes. The stained specimens were then dehydrated again by dipping in increasing concentrations of ethyl alcohol in water, cleared using Shandon Bluing Reagent (Thermo Scientific) for 1 minute and counterstained with Shandon Eosin Y Cytoplasmic Counterstain (Thermo Scientific) for 30 seconds. Again, each specimen was serially dehydrated in increasing concentrations of ethyl alcohol and then fixed in Histo-Clear (National Diagnostics). Sections were imaged under a light microscope to assess lumenal cross sectional area. A Nikon ECLIPSE Ti fluorescence microscope with a CoolSNAP photometrics camera was used to assess elastin deposition (48).

RNA Isolation /Real-Time Quantitative RT-PCR:

Total RNA was isolated from aortic tissue using Ambion's RiboPure kit. Tissues were harvested from AGS3 -/- and wild type mice, snap frozen in liquid nitrogen, and ground to a fine powder with a chilled mortar and pestle. Ground tissue samples were collected, reconstituted in Ambion's proprietary "TRI" reagent, subjected to 5 rounds of freeze/thawing, and centrifuged at 12,000 x g for 20 minutes at 4 °C. RNA was isolated from the supernatants by adding 200 µl of chloroform and centrifuging at 12,000 x g for 15 minutes at 4° C. RNA was precipitated from the aqueous layer by addition of 200 µl of 100% ethanol, collected by centrifugation, transferred to Ambion's provided filter columns, and finally eluted with 40 µl of sterile water. Purified RNA was stored at -80 °C.

cDNA Synthesis:

cDNA was synthesized in thin-walled PCR tubes by mixing 2 µg of total

RNA with 10 µl of RT master mix consisting of: 2 µl of 10x RT buffer, 2 µl of 10x random hexamers, 0.8 µl of 100 µM dNTP, 1 µl of RNAse inhibitor, 1 µl (200 units) of Superscript reverse transcriptase and 3.2 µl of water. The reaction mixture was incubated at 37° C for 150 minutes.

qRT-PCR:

Eight µl of PCR master mix (400 nM forward and reverse primers (IDT, Coralville, IA), 100 nM fluorogenic probe (Biosearch Technologies, Novato, CA), 5 mM $MgCl_2$, 200 µM deoxynucleotides, PCR buffer, and 1.25 units of Taq polymerase (Invitrogen) were added to wells of a 96-well plate containing 2 ul of each synthesized cDNA. Each 96-well plate reserved wells for an 18S probe as a standard for data normalization, and a no-template control well for each probe to account for non-specific fluorescence. All reactions were performed in triplicate using the following cycling conditions in a Mastercycler ep realplex real-PCR system (Eppendorf): 95 °C, 1 minute; followed by 40 cycles of 95 °C, 12 seconds, and 60 °C, 30 seconds.

Statistical Analysis:

Results are expressed as mean ± SD, unless indicated otherwise. One-way analysis of variance, followed by Turkey's post-hoc test was used for comparisons of hemodynamic time-course following DEA-NO and BAY41-2272 treatments. $P < 0.05$ was considered significant.

RESULTS:

I hypothesized that AGS3 acts as a negative modulator of sGC, and that an absence of AGS3 should increase sGC activity and function in tissues. To test this hypothesis I used an AGS3-defecient mouse model that was made available to us by Dr. Stephen Lanier at the Medical University of South Carolina. A knockout mouse line allows the investigator to better understand the role of the missing gene product by noting any phenotypic deviations compared to wild type mice, and by corroborating these observations with biochemical assays. In our case we thought that it was important to obtain an AGS3 knockout mouse line as a means to elucidate the changes of physiological and biochemical function of sGC in native tissues. With permission from Dr. Stephen Lanier, an AGS3-null mouse colony was established and maintained at the University of Texas Health Science Center's Animal Core Facility. Before evaluating the changes in sGC activity and function that may be caused by the lack of AGS3 protein, we confirmed the knockout of the AGS3 gene in the mice that were bred in our Animal Facility. As shown in Figure 7, genomic PCR confirmed the deletion of exon 3 of $AGS3^{-/-}$.

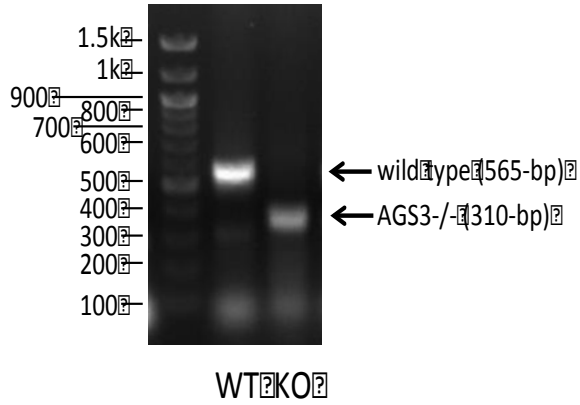

Figure 7. PCR genotyping of AGS3-/- (KO) and wild type mice. The expected 565-bp WT band was amplified from a WT mice ear sample, whereas the KO mouse sample exhibited instead a single 310-bp band, reflecting the loss of exon 3.

LGN/AGS3 – Since previous studies demonstrated that LGN and AGS3 proteins have similar effects on sGC function in vitro, we set out to test whether LGN might be up regulated to compensate for the lack of AGS3 protein in AGS3$^{-/-}$ mice. Therefore, a Western blot analysis was used to assess the levels of LGN in lung and aortic tissue from AGS3$^{-/-}$ and wild type mice. As shown in Figure 8, we found equivalent amounts of LGN in lung tissue for both wild type and AGS3$^{-/-}$ mice. However, we found no LGN signal in aortic tissue. This observation is consistent with the studies by the Lanier group, who evaluated the expression of LGN and AGS3 in a variety of mouse tissues (49). They found that the two proteins are differently expressed between tissues. Results in Figure 8 suggest that LGN expression was not increased in AGS3-deficient mice. A similar

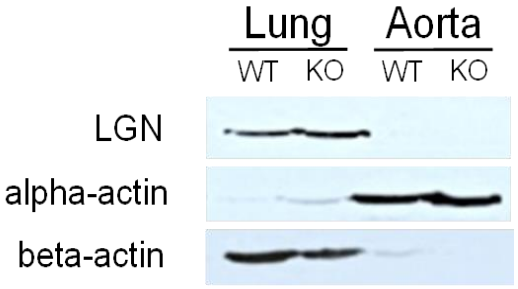

Figure 8. Expression of LGN protein is not detected aortas and is not increased in AGS3$^{-/-}$ mice. Lung and aortic tissue from wild type and AGS3$^{-/-}$ mice were homogenized and immunoblotted for the presence of LGN in cytosolic fractions.

conclusion can be drawn from results of RT-qPCR assays probing for AGS3 and LGN in aortic tissue samples from AGS3$^{-/-}$ and wild type mice (Fig. 9). LGN transcript levels were roughly equal between AGS3$^{-/-}$ and wild type mice (Fig. 9B). The lack of compensatory changes in LGN in aorta of AGS3$^{-/-}$ mice suggests that aorta may be a good tissue to investigate the effects of AGS3 knockout on the function and activity of sGC. Additionally, RT-qPCR was able to confirm that the level of AGS3 transcript in aortic tissue samples of AGS3$^{-/-}$ mice was only 4%

of that in its wild type counterpart (Fig. 9A). In summary, we confirmed the AGS3$^{-/-}$ knockout at the gene and transcript level. Moreover, we demonstrated a lack of compensatory expression of homologous LGN protein in the aorta, ruling out functional redundancy.

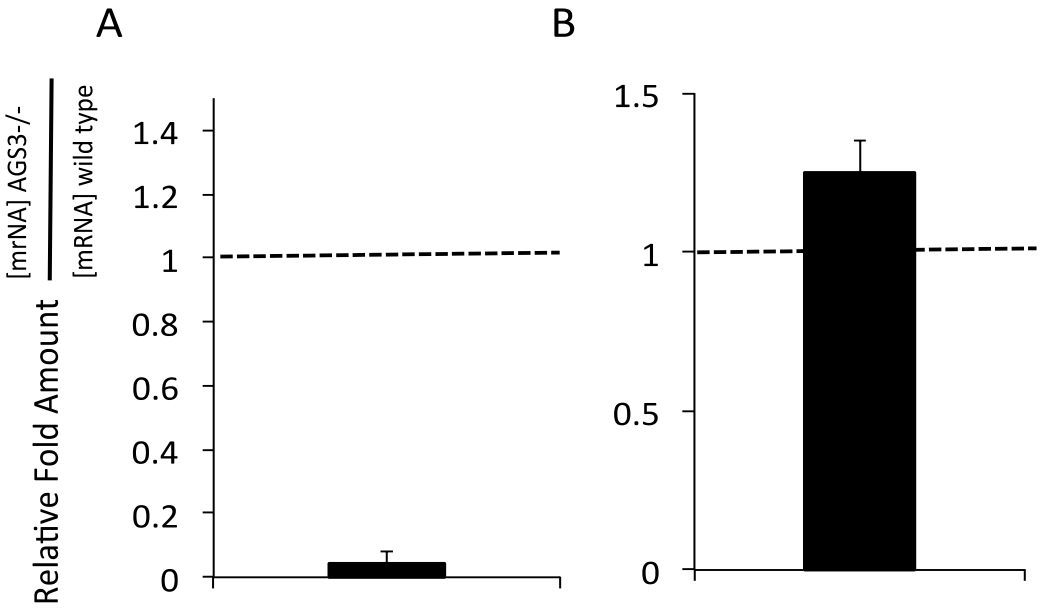

Figure 9. Comparison of LGN and AGS3 transcript level in AGS3$^{-/-}$ and wild type mice aorta lysates. The levels of AGS3 and LGN transcripts were determined by qRT-PCR and normalized to 18S ribosomal RNA to obtain ΔCT values, where $\Delta CT = CT_{AGS3-/-} - CT_{18S}$. Relative fold change in transcript levels for AGS3 (**A)** and LGN (**B)** were calculated based on ΔΔCT values, where $\Delta\Delta CT = \Delta CT_{AGS3-/-} - \Delta CT_{WT}$. Dashed line across graph demarcates equal transcript levels between AGS3$^{-/-}$ and wild type. Data represented as Mean ± SD (n=3)

Aim1: sGC Dependent Regulation of Blood Pressure in AGS3$^{-/-}$ Mice

To assess the effects of AGS3-deficiency on sGC-mediated regulation of blood pressure, we measured hemodynamic changes in wild type and AGS3$^{-/-}$ mice in response to NO-dependent and NO-independent sGC activators. First, we evaluated the resting blood pressure of both AGS3$^{-/-}$ and wild type mice. As shown in Figure 10, we found that AGS3$^{-/-}$ mice have a lower resting blood pressure in AGS3$^{-/-}$ mice than in wild-type counterparts. This observation is in line with previous results by Blumer et al, who recorded a 117 mmHg MABP for wild type mice and a 107 mmHg MABP for AGS3$^{-/-}$ animals (47).

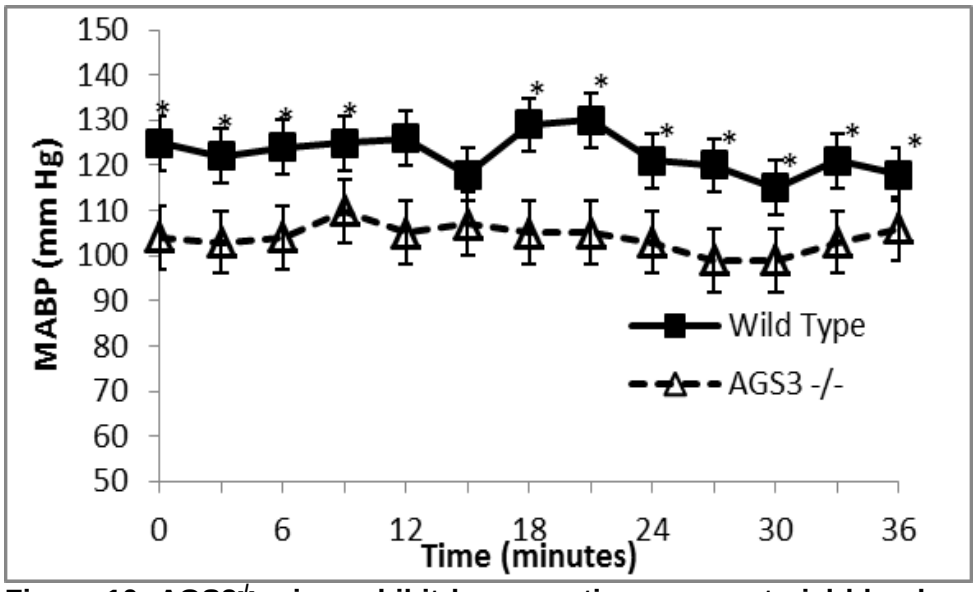

Figure 10. AGS3$^{-/-}$ mice exhibit lower resting mean arterial blood pressure (MABP) compared to wild type mice. MABP in wild type and AGS3$^{-/-}$ mice was monitored over a 36-minute period. Data presented as mean +/- SD (n = 10, WT; n = 16, AGS3-/-); *p <0.05.

Hemodynamic response to sGC activators - Next, blood pressure changes in wild type and AGS3$^{-/-}$ mice were monitored following IP-administration of two different sGC activators. First, we recorded the changes in blood pressure

following injection of DEA-NO, a chemical compound that releases NO while in circulation and mimics the endogenous production of NO. MABP changes were monitored over a 20-minute period to detect the maximal change in blood pressure, and the time required for restoration of blood pressure. As shown in Figure 11, AGS3$^{-/-}$ mice initially responded with a slightly larger, but not statistically significant, decrease in blood pressure following DEA-NO

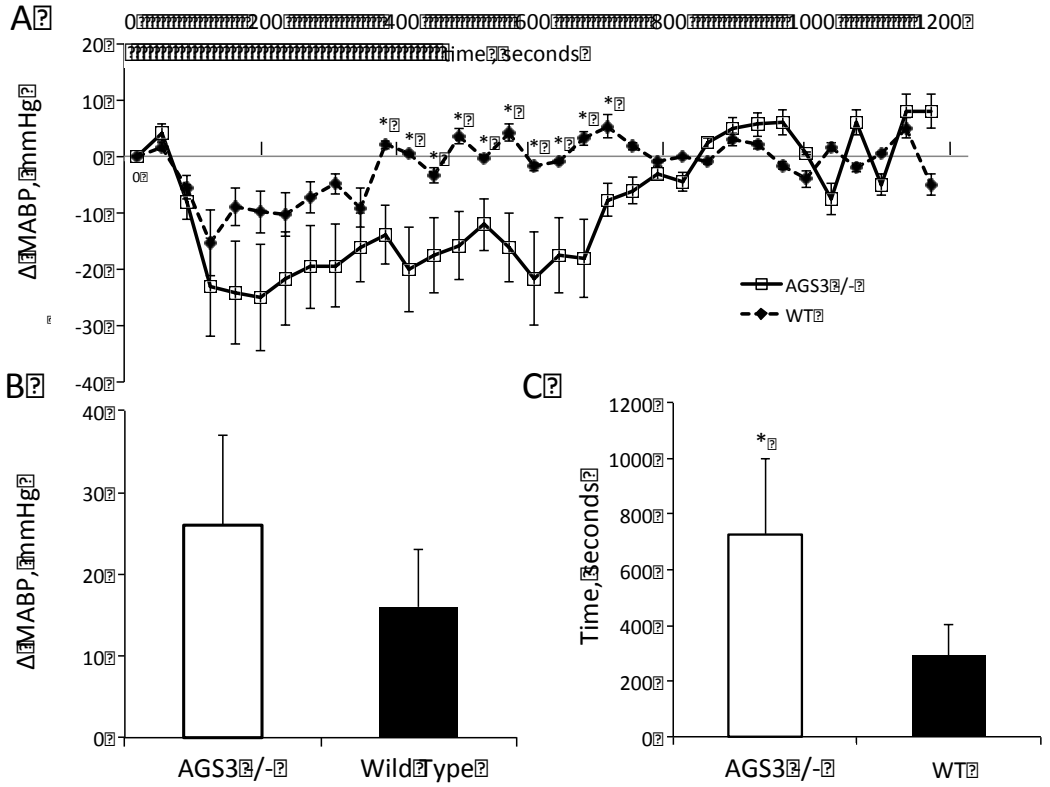

Figure 11. sGC-dependent vasomotor function is elevated in AGS3$^{-/-}$ animals following DEA-NO administration. **(A)** Changes in MABP in AGS3$^{-/-}$ and wild type mice following a single DEA-NO (80 g/kg) IP injection. MABP was non-invasively measured using the CODA system (Kent Scientific). **(B)** Maximal change in MABP following DEA-NO injection. **(C)** Time required to restore 80% of MABP following DEA-NO injection. Data are presented as mean+/- SE (n = 7). * $p < 0.01$.

administration compared to wild type mice (Fig. 11A, B). We observed that AGS3$^{-/-}$ mice maintained the decreased blood pressure much longer than the wild type controls (Fig. 11A, C). We also probed the mice with an NO-independent sGC activator, BAY41-2272. The use of an NO-independent sGC activator allows us to determine if the effects of DEA-NO may be attributed to sGC-independent effects of NO. The results presented in Figure 12 indicate that AGS3$^{-/-}$ mice experience a much larger decrease in the MABP (Fig. 12B), and require longer times to restore MABP to initial values (Fig. 12C). In conclusion, the sGC-dependent decreases in blood pressure by BAY41-2272 and by NO were more pronounced in AGS3 deficient mice.

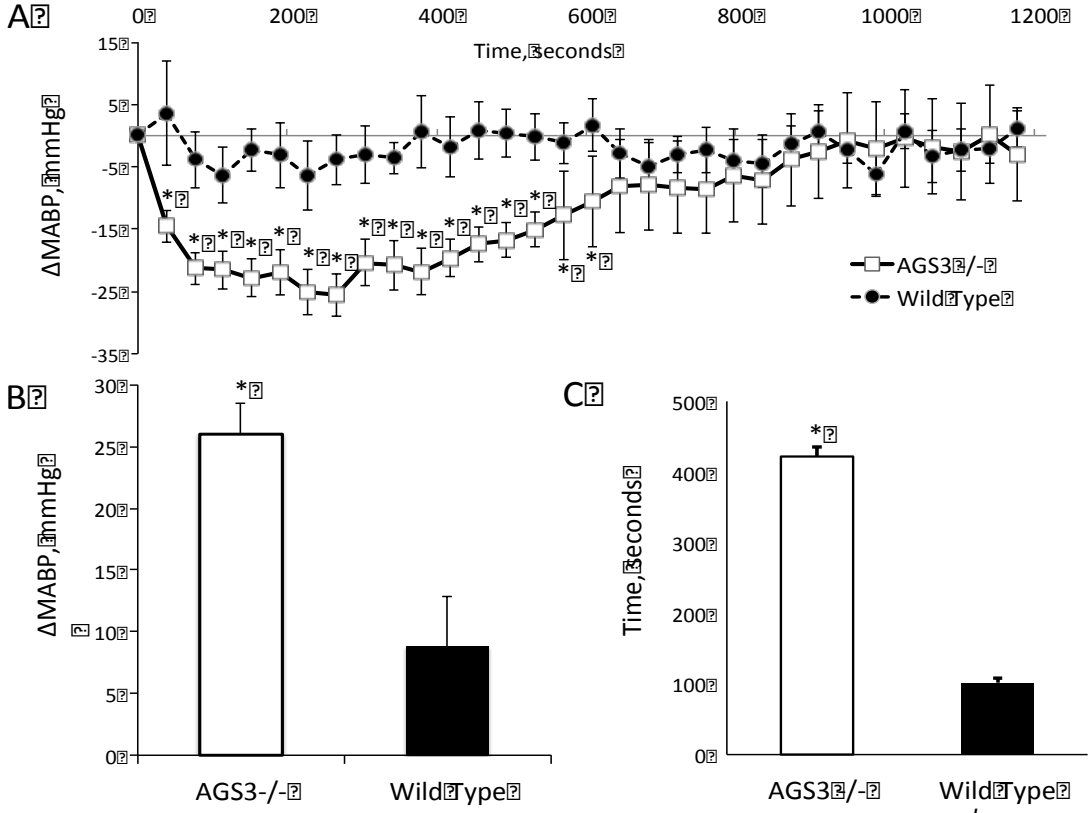

Figure 12. **sGC dependent vasomotor function is elevated in AGS3$^{-/-}$ animals following BAY41-2272 administration**. **(A)**: Changes in blood pressure in AGS3$^{-/-}$ and wild type mice following a single IP injection of BAY41-2272 (200 µg/kg). MABP were non-invasively measured using the CODA system. **(B)** Maximal change in the MABP following BAY41-2272. **(C)** Time required to restore 80% MABP following BAY41-2272. Data are presented as mean +/- SE (WT n = 10; AGS3-/- n = 16). *p<0.01.

Histology of Blood Vessels - To check whether the differences between the mouse strains might have been a result of vascular anatomical variations between AGS3$^{-/-}$ and wild type mice, descending aortas from each strain was excised and sectioned for H&E staining and autofluorescence detection. H&E staining allowed proper distinctions to be made between smooth muscle and adventitia of the vessel, which allowed cross sectional area quantifications to be made for the lumen and the media layer containing vascular smooth muscle cells. This provided a means to separately measure lumenal and whole vessel cross sectional areas for each section. The data was normalized by calculating a ratio of the cross sectional areas of the lumen and the whole vessel (Fractional lumen cross section). The fractional lumenal cross sections in AGS3$^{-/-}$ and wild type mice were roughly similar (Fig. 13A and B).

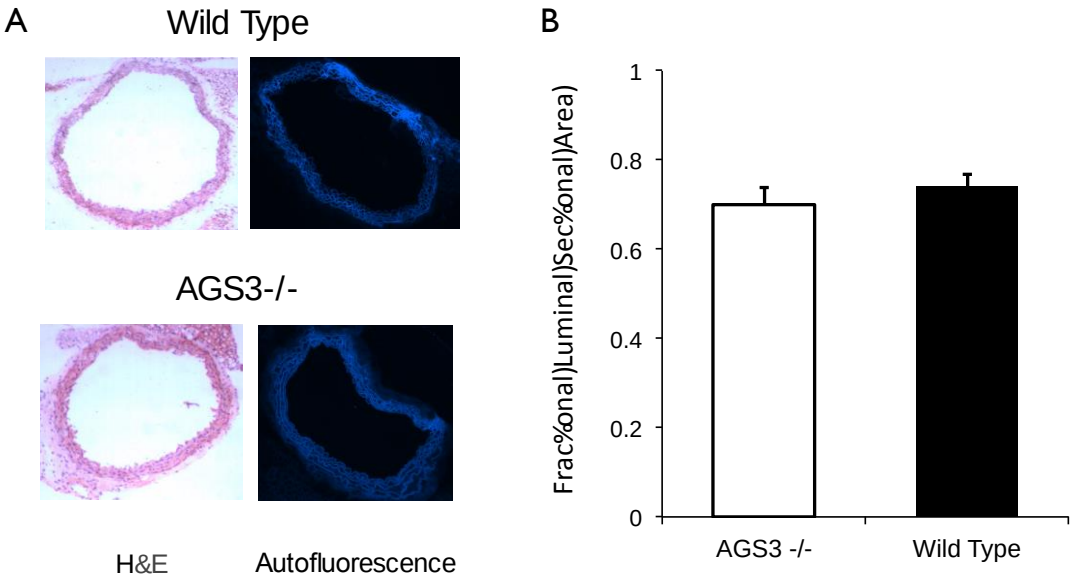

Figure 13. Wild type and AGS3$^{-/-}$ mice blood vessel structure. (A) Four sections per mouse (n=6) were stained with H&E to visualize the anatomy of blood vessels (left panels). Four sections per mouse (n=6) were used to assess the extracellular matrix in the vascular wall by monitoring the autofluorescence of elastin (right panels). **(B)** Fractional luminal sectional area was determined from H&E sections by taking the ratio of the luminal area in the section to the area of the whole vessel. Data is presented as mean +/- SD based on 24 sections from 6 mice per group (n=24).

An elevated deposition of the extracellular matrix may significantly affect the vasorelaxing properties of blood vessels (48). Therefore, we also assessed the deposition of extracellular matrix in the aortas of AGS3$^{-/-}$ and wild type mice. We took advantage of the autofluorescence of elastin in the vascular tissue to assess whether significant changes in matrix structure or amount occurred due to AGS3 deficiency. As shown in Figure 13A (right panels), images acquired with a FITC filter did not reveal any differences in matrix structure or amount between wild type and AGS3$^{-/-}$ mice. These data on lumen and matrix dimensions allowed us to conclude that there were no gross distortions in the structural elements in the vessels that may directly affect the vasomotor function in AGS3$^{-/-}$ mice.

Previous studies demonstrated that totally sGC deficient mice develop hypertension (50). Moreover, mice that lack sGC only in vascular smooth muscle cells also develop hypertension (50,51), indicating that sGC-dependent regulation of blood pressure is contributed predominantly by the vascular smooth muscle cells. Thus, the data presented above suggest that changes in the hemodynamic parameters in response to sGC agonists in AGS3$^{-/-}$ mice may be attributed to changes in sGC vasomotor function in the vascular bed.

Aim2: sGC activity in AGS3$^{-/-}$ mice

The main goal of this aim was to determine if sGC activity was changed in the aortic tissue of AGS3$^{-/-}$ mice. Before directly testing this hypothesis, we set to rule out some processes that may indirectly affect the activity of sGC in AGS3$^{-/-}$ mice including changes to the PDE activity and altered sGC expression.

PDE Activity - Decreased PDE-dependent hydrolysis of cGMP may significantly enhance the vascular response to sGC targeting agents without affecting sGC activity. Thus, we assessed whether the absence of AGS3 expression altered PDE activity. Aortic tissue lysates from AGS3-/- and wild type mice were incubated with [^{32}P] cGMP, as described in Methods. The representative chromatogram in Figure 14A illustrates the procedure for quantitating PDE activity in lysates with or without a PDE inhibitor. The reaction product [^{32}P] GMP was separated from the substrate [^{32}P] cGMP using TLC, as described in Methods. The intensity of the [^{32}P] GMP was quantified by densitometry to determine the amount of generated GMP. We found that similar amounts of AGS3$^{-/-}$ lysate produced ~50% more [^{32}P] GMP than the wild type lysates, indicating an elevated PDE activity in the AGS3$^{-/-}$ tissue (Fig. 14A). The use of PDE inhibitors allowed us to confirm that the observed conversion of cGMP to GMP was due to PDE activity. Figure 14B shows the rate of GMP formation in the presence of PDE5 specific inhibitor (Sildenafil) and a general PDE inhibitor, IBMX. Interestingly, in wild type mice the overall PDE activity may be contributed primarily by PDE5, as sildenafil and IBMX inhibitions were PDE

statistically indistinguishable. However, in AGS3$^{-/-}$ mice, the nonspecific PDE inhibitor (IBMX) provided significantly more PDE inhibition than Sildenafil, suggesting that one or more other PDEs may be up-regulated in AGS$^{-/-}$ mice. In summary, PDE activity actually increases in AGS3$^{-/-}$ mice so altered PDE activity cannot explain the enhanced sGC dependent function observed in the AGS3$^{-/-}$ mice.

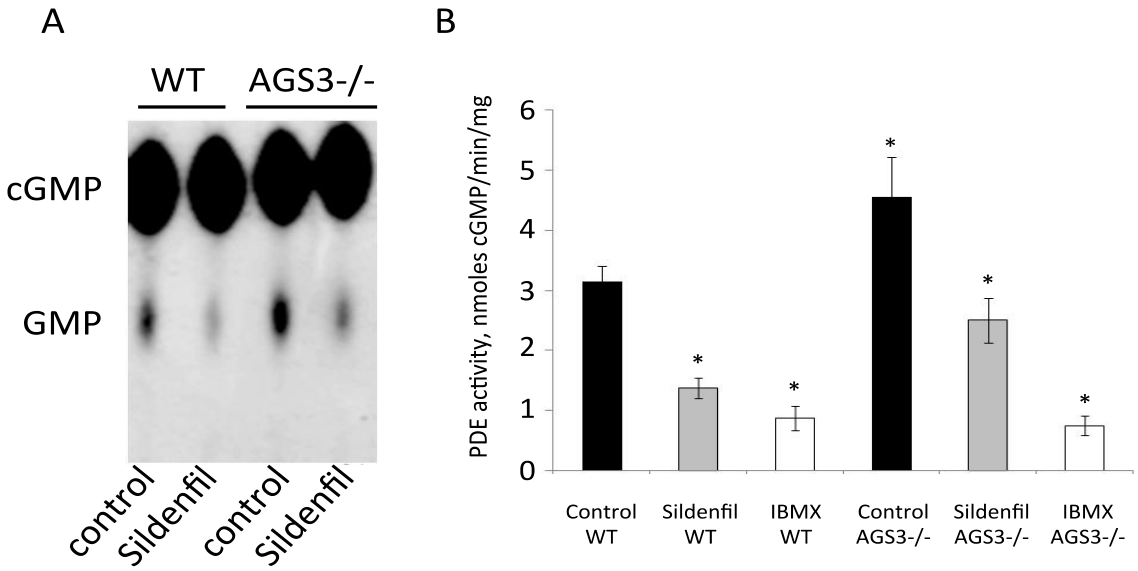

Figure 14. Phosphodiesterase (PDE) activity in aortic lysates of AGS3$^{-/-}$ and wild type mice. cGMP [α-^{32}P] was synthesized using purified sGC and was incubated with mouse aortic lysates in the presence of PBS, specific PDE5 inhibitor Sildenafil, or nonspecific PDE inhibitor IBMX. Reaction products were separated by TLC on polyethyleneimine cellulose TLC plates. **(A)** A representative TLC radiochromatogram with substrate and product of PDE reaction indicated. **(B)** PDE activity in aortic lysates of wild type and AGS3$^{-/-}$ in the presence of vehicle (PBS), Sildenafil or IBMX. Data are presented as mean +/- SD (n=6). * $p<0.05$.

sGC Subunit Expression in AGS3$^{-/-}$ Mice - Increased expression of sGC protein in AGS3$^{-/-}$ also might explain the observed enhancement of the sGC-dependent hemodynamic response. To test this, a Western blot analysis was performed on aortic tissues. The cytosolic fractions expected to contain sGC were separated by SDS-PAGE and probed with antibodies against the α1 or β1

subunits of sGC. The results shown in Figure 15A demonstrate that very similar amounts of the β1 subunit are found in aorta cytosol of both AGS3$^{-/-}$ and wild type mice. However, substantially less α1 subunit was observed in the aorta from AGS3$^{-/-}$ mice (Fig. 15A). As translocation of α1 sGC to membrane compartments

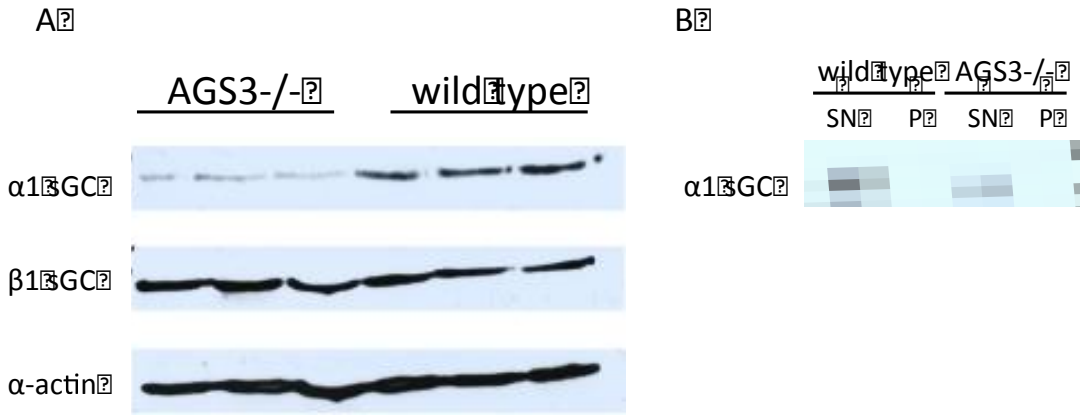

Figure 15. Expression of sGC subunits in AGS3$^{-/-}$ and wild type mice. (A) Expression of α1 and β1 sGC subunits in cytosolic fractions of AGS3$^{-/-}$ and wild type aortic lysates was probed by Western blotting using antibodies against α1 and β1 of sGC subunits. α-actin was used to assess equal loading. **(B)** α1 sGC does not translocate to the membranes. High-speed supernatants (Sn) and pellets (P) from wild type and AGS3$^{-/-}$ aortic tissues were separated by ultracentrifugation and probed for α1 sGC by Western blotting.

might explain the decrease in the cytosolic α1 levels, we assessed the amounts of α1 in the membrane fractions. As shown in Figure 15B, α1 proteins was not observed in the 100,000 x g pellets (membrane fraction) from either wild type or AGS3$^{-/-}$ aortas. Thus, translocation to the membrane does not occur to any significant extent and there is actually an overall decrease in α1 protein levels in aortas of AGS3$^{-/-}$ mice.

Next, we looked for possible differences in transcription in AGS3$^{-/-}$ and wild type mice that might explain the differences in α1 protein levels between the mice strains. RT-qPCR was utilized to measure the relative abundance of α1 mRNA in aortic samples from AGS3$^{-/-}$ and wild type mice (Fig 15A). We found

that wild type and AGS3$^{-/-}$ samples contained comparable levels of α1 sGC transcript. This means that differences in α1 protein level are not due to differences in α1 message levels.

Previous reports have noted increased amounts of α2 protein in aortas of α1 knockout mice (52). Thus, we looked for changes in α2 transcript level in the AGS3$^{-/-}$ mice. As shown in Figure 16, we found that AGS3$^{-/-}$ mice had essentially unchanged transcript levels for α1, α2 or β1 sGC subunits. This implies that there was no compensation of α1 loss through increased transcription and translation of the α2 sGC subunit in aorta of the AGS3$^{-/-}$ mice. As sGC is an obligate

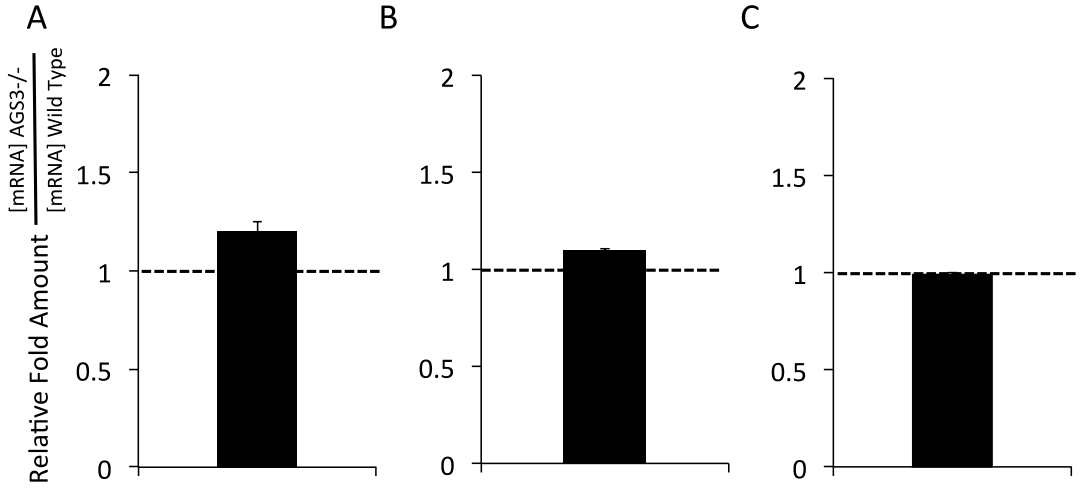

Figure 16. Level of sGC transcripts in AGS3$^{-/-}$ and wild type mice. Transcript levels of α1, β1 and α2 were determined by qRT-PCR and normalized to 18S ribosomal RNA to obtain ΔCT values, where $\Delta CT = CT_{target} - CT_{18S}$. Relative fold change in transcript levels for α1 **(A)**, β1 **(B)** and α2 **(C)** were calculated based on ΔΔCT values, where $\Delta\Delta CT = \Delta CT_{target} - \Delta CT_{WT}$. Dashed line across graph demarcates equal transcript levels between AGS3$^{-/-}$ and wild type samples. Data are presented as mean ± SD (n=3).

heterodimer, the observed decrease in α1 protein levels implies a lower amount of functional sGC in the AGS3 knockout animals. In conclusion, the enhanced sGC-dependent response observed in AGS3$^{-/-}$ mice is not the result of increased

sGC expression in these animals.

sGC Activity - Next, we sought to directly assess sGC activity in AGS3$^{-/-}$ mice. We measured the accumulation of [^{32}P] cGMP in aortic tissue cytosol incubated with [α-^{32}P] GTP, in the presence or absence of an NO-donor, DEA-NO. Similar to the PDE assay, the reaction products were separated by TLC and the amount of [^{32}P] cGMP formed was quantified. Previously preformed controls validated the position of GTP, cGMP and GMP along the vertical axis of the TLC plate (not shown). As expected, DEA-NO increased sGC activity in both AGS3$^{-/-}$ and wild type mice (Fig 17A,B). However, we found that the same amount of AGS3$^{-/-}$ lysate total protein generated more cGMP in response to NO than did the wild type lysate (Fig. 17A). To take into account the difference in the expression of functional heterodimeric sGC between AGS3$^{-/-}$ and wild type mice, sGC conversion rates were normalized to the expression of the α1 subunit and

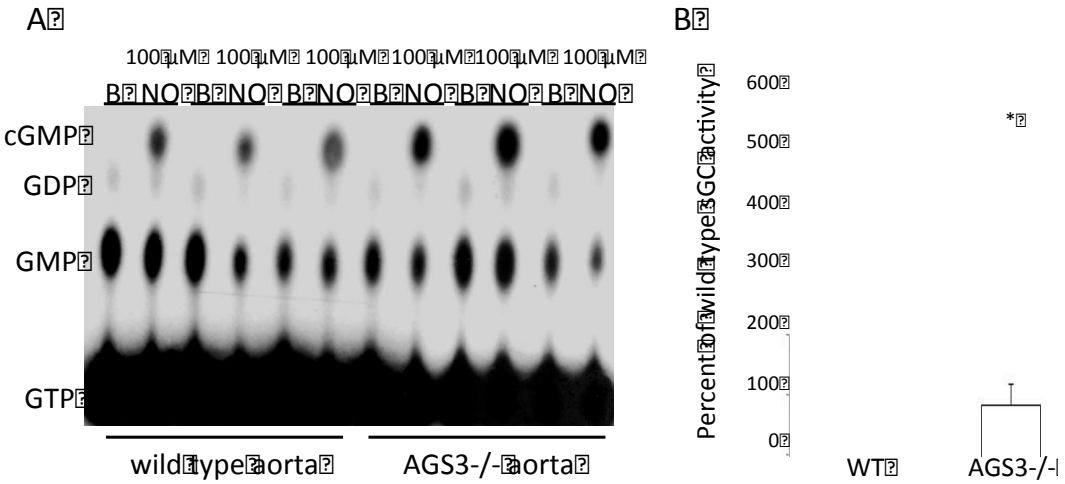

Figure 17. sGC activity is elevated in AGS3$^{-/-}$ aorta lysates. GTP [α-^{32}P] was incubated with equal amounts of wild type and AGS3$^{-/-}$ mouse aortic lysates in the presence of PBS (B), or 100 µM DEA-NO (NO). Reaction products were separated on a polyethyleneimine cellulose TLC plate and visualized by radiography. **(A)** A representative TLC radiochromatogram with the positions of substrate (GTP) and product (cGMP) of the sGC reaction indicated. GMP and putative GDP positions are also indicated. **(B)** The quantity of cGMP was determined by densitometry and used to calculate relative sGC activity in wild type and AGS3$^{-/-}$ mice. Data are presented as mean +/- SD (n=3) *p<0.05.

reported as the percent of wild type sGC activity. As presented in Figure 17B, this analysis indicated that relative specific activity of sGC in AGS3$^{-/-}$ mice was nearly 5 times higher than in the wild type mice. These results strongly indicate that the absence of AGS3 protein lead to an inherently more active sGC. In summary, these data clearly are consistent with our hypothesis that AGS3 is a negative modulator of sGC in vivo.

DISCUSSION:

As previously mentioned, the NO/sGC/cGMP pathway has significant cardiovascular implications. Activation of the pathway is known to be beneficial for atherosclerosis, thrombosis, or stroke patients by inhibiting platelet adhesion to vascular endothelium (53)and/or by relaxing smooth muscle cells to reduce blood pressure (54). However, in the pathological state, NO bioavailability is reduced by its interaction with the increase in abundance of reactive oxygen species generated by surrounding inflammatory processes (55). As a result, NO-dependent activation of sGC is compromised, and unable to mediate vasodilation. Currently, NO-donors (glyceryl trinitrate, isosorbide nitrates) are used as pharmacological agents to supplement the loss of endogenous NO levels that are ultimately thought to mitigate vasoconstriction in patients experiencing angina (56). Unfortunately, research has shown that these patients develop tolerance over time, limiting the efficacy of this treatment method (57). Elevated levels in circulating NO from exogenous treatment sources, react with local reactive oxygen species to further curb NO availability, and to further increase oxidative stress (58). Moreover, elevated oxidative stress results in the oxidation of sGC, rendering it unresponsive to available NO (58). Therefore, there is a growing need in the clinic for methods that implement NO-independent activation of sGC to manage cardiovascular diseases. With this category of drug, oxidative stress stemming from NO-donor treatment could be minimized. The list of agents that have been identified to activate sGC without the use of NO has expanded in recent years. Nevertheless, many of these compounds are found to

be toxic *in vivo* (59). As a result, alternative for a safe and effective treatment method for stimulating sGC are needed.

In this study, we show that AGS3 deficiency in mice resulted in increased duration of sGC-mediated vasodilation compared to wild type mice, which could be attributed to increased activity of sGC in aorta. These studies describe an AGS3 function outside its accepted role as a receptor-independent activator of G-protein signaling, highlighting its action in modulating sGC function.

To gain insight into the possible changes in sGC function, an AGS3 knockout colony was obtained from Dr. Stephen Lanier, whose group generated these mice. We believed this was a strong approach that allowed us to directly assess the changes in sGC activity in the absence of endogenous AGS3. Generating a similar knockout model in fruit flies or yeast would have provided limited information regarding the effect of AGS3 on sGC.

Once we had confirmed the mice were indeed AGS3 null, we monitored and compared hemodynamic responses to sGC activators in AGS3$^{-/-}$ and wild type mice. Administration of either an NO-dependent (DEA-NO) or an NO-independent activator (BAY41-2272) of sGC in AGS3$^{-/-}$ mice resulted in extended depression in the mean arterial blood pressure as compared to wild type mice. Our direct measurements of sGC activity indicated that the activity was nearly five times higher in AGS3$^{-/-}$ mice than in the wild-type counterparts. These results led us to infer that elevated sGC activity sustains the decrease in the mean arterial blood pressure. The confluence of results from *in vivo* blood pressure monitoring and *in vitro* biochemical assays in the present study support my

hypothesis that AGS3 operates as a negative modulator of sGC function. To ensure that NO-dependent signaling processes function properly, the rise and fall of intracellular cGMP levels in response to NO should be tightly regulated. AGS3-dependent inhibition of sGC may contribute to this regulation.

Unexpectedly, we discovered that AGS3$^{-/-}$ deficient mice express a lower level of α1 sGC subunit in aorta as compared to their wild-type counterparts. Although our studies demonstrated that this decrease is not due to changes in α1 transcription, it remains to be determined if the exact cause involves translational control, ubiquitin-mediated protein degradation, or post-transcriptional regulation by microRNAs. Secondary to this observation, we were interested in understanding why the level of β1 sGC subunit protein did not decrease together with α1. Traditionally, unbound subunits of a larger complex of proteins become unstable and are targeted for proteolysis. However, our after observation of an imbalance in sGC subunit expression in aortas of AGS3$^{-/-}$ mice appears to counter this notion. Literature analysis identified a study by Zabel et al (60), which tested whether sGC subunits are capable of forming homodimers intracellularly. They demonstrated that both α1 and β1 subunits form stable homodimers in the absence of the opposite subunit. It is thus reasonable to consider that the β subunit of sGC in AGS3$^{-/-}$ mice escapes degradation due to homodimerization.

The proposed role of AGS3 as a negative modulator of sGC activity has important implications ifor regulating sGC function. Current regulators of sGC function that are considered for applications in a clinical setting are NO

generators, or NO-independent sGC activators targeting an sGC allosteric site. The existing approaches do not include alternative modes of regulating sGC function. Namely, little efforts have been focused on identifying and down regulating endogenously produced agents involved in deactivating sGC. As a start to filling this gap, we provide evidence that removing AGS3 expression in vascular smooth muscle tissue results in slower sGC deactivation and more sustained blood vessel dilation.

The exact mechanism of AGS3-dependent inhibition of sGC remains uncharacterized. In a previous study conducted by Chauhan and colleagues (46), it was demonstrated that activated sGC was inhibited in the presence of AGS3. It remains to be determined whether a direct interaction between sGC and AGS3 is required. Co-immunoprecipitation experiments with purified proteins might be conducted to test for direct interaction between AGS3 and sGC. As mentioned previously, AGS3 is highly similar to LGN protein, a proven direct sGC interactor (43). Furthermore, that study demonstrated that sGC-LGN interaction results in inhibition of sGC activity. Mapping the region of interaction between sGC and LGN revealed that the TPR-containing domain of LGN is sufficient for interaction with the catalytic domain of sGC (46). Because of the high degree of amino acid sequence homology (70%) between AGS3 and LGN in the TPR domain (aa 1-390), it is reasonable to assume that AGS3 also binds and interacts with sGC at the catalytic domain to inhibit its function. Elevated sGC activity and function in AGS3-/- mice may also be explained by increased stability of the sGC-NO complex. As described above, once NO dissociates from sGC the production of

cGMP falls to a basal state. In future studies, this hypothesis might be tested by direct spectroscopic analyses of the stability of sGC-NO complex in the absence and presence of purified AGS3.

Future studies will also need to be performed to determine whether AGS3 alone is sufficient for sGC deactivation, or if additional cellular factors are needed. Previous studies demonstrated that AGS3 can bind with more than one protein simultaneously (42). For example, the GoLoco domain of AGS3 is capable of binding several G_{α} subunits to coordinate distinct G-protein signaling pathways (61). This multivalent action is likely a result of the presence of multiple GPR motifs in the GoLoco domain. Previous studies also demonstrated that just one TPR motif is sufficient to mediate protein-protein interactions (62). Thus, AGS3, which contains seven TPR motifs, may potentially bind seven different target proteins. The linker region of LGN, located between the TPR and GoLoco domains, has also been shown to interact with postsynaptic density 95 (PSD95), synapse-associated protein 102 (SAP 102), and the serine/threonine kinase LKB1 (63), suggesting that this region of AGS3 may also bind to other proteins. All together, AGS3 may have the potential to function as a scaffolding protein and recruit accessory proteins into a larger complex that modulate sGC function. Further work is needed to determine the exact nature of any protein complex that associates with sGC. While the present studies revealed the effects of AGS3 deficiency in the vascular function of sGC, it remains to be determined whether sGC function is affected in other tissues. Of special interest are the lung and brain tissues, where high level of sGC and AGS3 has been previously

reported(46,49).

It also remains to be determined whether AGS3 interactions have additional cellular signaling implications. Originally found to bind and stabilize $G_{\alpha i}$ in the GDP state located in the cellular membrane(43), AGS3 effectively increases the production of cAMP from ATP in the cell. How might recruitment of AGS3 into a complex with activated sGC affect $G_{\alpha i}$ signaling? It has been previously reported that the membrane bound FERM and PDZ domain containing 1 protein (Frmpd1) localizes AGS3 to membrane fractions by its interaction with the TPR domain of AGS3 (64). These studies demonstrated that upon the cell receiving a stimulus, AGS3 might switch binding partners, altering the extent of its association with $G_{\alpha i}$. A similar process may be postulated for sGC-AGS3 interaction. Moreover, the putative scaffolding function of AGS3 and its association with membrane-bound proteins may affect the localization of sGC among various subcellular locations.

In conclusion, the present studies provide additional support to the hypothesis that AGS3 protein is a negative modulator of sGC function. While many aspects of the mechanism of action are not understood, this interaction may be the basis for a new type of regulation of sGC function in the cardiovascular system. One can envision a new type of drug that interferes with the interaction of AGS3 and sGC to modulate the inhibition of sGC by AGS3, thereby sensitizing the response of sGC to endogenous NO levels. Additionally, novel therapeutic interventions aimed at dilating blood vessels might be tailored to increase sGC activity targeted disruption of AGS3.

REFERENCES:

1. Rapoport, R. M., Draznin, M. B., and Murad, F. (1983) Endothelium-dependent relaxation in rat aorta may be mediated through cyclic GMP-dependent protein phosphorylation. *Nature* **306**, 174-176

2. Zhuo, M., and Hawkins, R. D. (1995) Long-term depression: a learning-related type of synaptic plasticity in the mammalian central nervous system. *Reviews in the neurosciences* **6**, 259-277

3. Moncada, S., and Higgs, E. A. (2006) The discovery of nitric oxide and its role in vascular biology. *British journal of pharmacology* **147 Suppl 1**, S193-201

4. Held, K. F., and Dostmann, W. R. (2012) Sub-Nanomolar Sensitivity of Nitric Oxide Mediated Regulation of cGMP and Vasomotor Reactivity in Vascular Smooth Muscle. *Frontiers in pharmacology* **3**, 130

5. Chan, J. Y., Chan, S. H., and Chang, A. Y. (2004) Differential contributions of NOS isoforms in the rostral ventrolateral medulla to cardiovascular responses associated with mevinphos intoxication in the rat. *Neuropharmacology* **46**, 1184-1194

6. Sato, J., Nair, K., Hiddinga, J., Eberhardt, N. L., Fitzpatrick, L. A., Katusic, Z. S., and O'Brien, T. (2000) eNOS gene transfer to vascular smooth muscle cells inhibits cell proliferation via upregulation of p27 and p21 and not apoptosis. *Cardiovascular research* **47**, 697-706

7. Balligand, J. L., Feron, O., and Dessy, C. (2009) eNOS activation by physical forces: from short-term regulation of contraction to chronic remodeling of cardiovascular tissues. *Physiological reviews* **89**, 481-534

8. Sessa, W. C. (2004) eNOS at a glance. *Journal of cell science* **117**, 2427-2429

9. Derbyshire, E. R., and Marletta, M. A. (2012) Structure and regulation of soluble guanylate cyclase. *Annual review of biochemistry* **81**, 533-559

10. Kass, D. A., Takimoto, E., Nagayama, T., and Champion, H. C. (2007) Phosphodiesterase regulation of nitric oxide signaling. *Cardiovascular research* **75**, 303-314

11. Bender, A. T., and Beavo, J. A. (2006) Cyclic nucleotide phosphodiesterases: molecular regulation to clinical use. *Pharmacological reviews* **58**, 488-520

12. Pauvert, O., Salvail, D., Rousseau, E., Lugnier, C., Marthan, R., and Savineau, J. P. (2002) Characterisation of cyclic nucleotide phosphodiesterase isoforms in the media layer of the main pulmonary artery. *Biochemical pharmacology* **63**, 1763-1772

13. Liu, X. M., Peyton, K. J., Wang, X., and Durante, W. (2012) Sildenafil stimulates the expression of gaseous monoxide-generating enzymes in vascular smooth

muscle cells via distinct signaling pathways. *Biochemical pharmacology* **84**, 1045-1054

14. Lincoln, T. M. (2007) Myosin phosphatase regulatory pathways: different functions or redundant functions? *Circulation research* **100**, 10-12

15. Ignarro, L. J. (1996) Physiology and pathophysiology of nitric oxide. *Kidney international. Supplement* **55**, S2-5

16. Francis, S. H., Busch, J. L., Corbin, J. D., and Sibley, D. (2010) cGMP-dependent protein kinases and cGMP phosphodiesterases in nitric oxide and cGMP action. *Pharmacological reviews* **62**, 525-563

17. Yao, X., Leung, P. S., Kwan, H. Y., Wong, T. P., and Fong, M. W. (1999) Rod-type cyclic nucleotide-gated cation channel is expressed in vascular endothelium and vascular smooth muscle cells. *Cardiovascular research* **41**, 282-290

18. Bruton, T., and Lauder. (1867) On The Use Of Nitrite of Amyl in Angina Pectoris. *The Lancet* **90**, 97-98

19. Murrell, and William. (1879) Nitro-Glycrine as a Remedy for Angina Pectoris. *The Lancet* **113**, 80-81

20. Andreopoulos, S., and Papapetropoulos, A. (2000) Molecular aspects of soluble guanylyl cyclase regulation. *General pharmacology* **34**, 147-157

21. Wang, H., Zhong, F., Pan, J., Li, W., Su, J., Huang, Z. X., and Tan, X. (2012) Structural and functional insights into the heme-binding domain of the human soluble guanylate cyclase alpha2 subunit and heterodimeric alpha2beta1. *Journal of biological inorganic chemistry : JBIC : a publication of the Society of Biological Inorganic Chemistry* **17**, 719-730

22. Russwurm, M., Wittau, N., and Koesling, D. (2001) Guanylyl cyclase/PSD-95 interaction: targeting of the nitric oxide-sensitive alpha2beta1 guanylyl cyclase to synaptic membranes. *The Journal of biological chemistry* **276**, 44647-44652

23. Bellingham, M., and Evans, T. J. (2007) The alpha2beta1 isoform of guanylyl cyclase mediates plasma membrane localized nitric oxide signalling. *Cellular signalling* **19**, 2183-2193

24. Koglin, M., and Behrends, S. (2003) A functional domain of the alpha1 subunit of soluble guanylyl cyclase is necessary for activation of the enzyme by nitric oxide and YC-1 but is not involved in heme binding. *The Journal of biological chemistry* **278**, 12590-12597

25. Zhao, Y., and Marletta, M. A. (1997) Localization of the heme binding region in soluble guanylate cyclase. *Biochemistry* **36**, 15959-15964

26. Wedel, B., Humbert, P., Harteneck, C., Foerster, J., Malkewitz, J., Bohme, E., Schultz, G., and Koesling, D. (1994) Mutation of His-105 in the beta 1 subunit yields a nitric oxide-insensitive form of soluble guanylyl cyclase. *Proceedings of*

the National Academy of Sciences of the United States of America **91**, 2592-2596

27. Henry, J. T., and Crosson, S. (2011) Ligand-binding PAS domains in a genomic, cellular, and structural context. *Annual review of microbiology* **65**, 261-286

28. Underbakke, E. S., Iavarone, A. T., Chalmers, M. J., Pascal, B. D., Novick, S., Griffin, P. R., and Marletta, M. A. (2014) Nitric oxide-induced conformational changes in soluble guanylate cyclase. *Structure* **22**, 602-611

29. Ma, X., Beuve, A., and van den Akker, F. (2010) Crystal structure of the signaling helix coiled-coil domain of the beta1 subunit of the soluble guanylyl cyclase. *BMC structural biology* **10**, 2

30. Tesmer, J. J., Sunahara, R. K., Gilman, A. G., and Sprang, S. R. (1997) Crystal structure of the catalytic domains of adenylyl cyclase in a complex with Gsalpha.GTPgammaS. *Science* **278**, 1907-1916

31. Pyriochou, A., and Papapetropoulos, A. (2005) Soluble guanylyl cyclase: more secrets revealed. *Cellular signalling* **17**, 407-413

32. Harteneck, C., Koesling, D., Soling, A., Schultz, G., and Bohme, E. (1990) Expression of soluble guanylyl cyclase. Catalytic activity requires two enzyme subunits. *FEBS letters* **272**, 221-223

33. Campbell, M. G., Underbakke, E. S., Potter, C. S., Carragher, B., and Marletta, M. A. (2014) Single-particle EM reveals the higher-order domain architecture of soluble guanylate cyclase. *Proceedings of the National Academy of Sciences of the United States of America* **111**, 2960-2965

34. Batchelor, A. M., Bartus, K., Reynell, C., Constantinou, S., Halvey, E. J., Held, K. F., Dostmann, W. R., Vernon, J., and Garthwaite, J. (2010) Exquisite sensitivity to subsecond, picomolar nitric oxide transients conferred on cells by guanylyl cyclase-coupled receptors. *Proceedings of the National Academy of Sciences of the United States of America* **107**, 22060-22065

35. Bellamy, T. C., Wood, J., Goodwin, D. A., and Garthwaite, J. (2000) Rapid desensitization of the nitric oxide receptor, soluble guanylyl cyclase, underlies diversity of cellular cGMP responses. *Proceedings of the National Academy of Sciences of the United States of America* **97**, 2928-2933

36. Meurer, S., Pioch, S., Wagner, K., Muller-Esterl, W., and Gross, S. (2004) AGAP1, a novel binding partner of nitric oxide-sensitive guanylyl cyclase. *The Journal of biological chemistry* **279**, 49346-49354

37. Ghosh, A., and Stuehr, D. J. (2012) Soluble guanylyl cyclase requires heat shock protein 90 for heme insertion during maturation of the NO-active enzyme. *Proceedings of the National Academy of Sciences of the United States of America* **109**, 12998-13003

38. Balashova, N., Chang, F. J., Lamothe, M., Sun, Q., and Beuve, A. (2005) Characterization of a novel type of endogenous activator of soluble guanylyl cyclase. *The Journal of biological chemistry* **280**, 2186-2196

39. Heckler, E. J., Crassous, P. A., Baskaran, P., and Beuve, A. (2013) Protein disulfide-isomerase interacts with soluble guanylyl cyclase via a redox-based mechanism and modulates its activity. *The Biochemical journal* **452**, 161-169

40. Hanafy, K. A., Martin, E., and Murad, F. (2004) CCTeta, a novel soluble guanylyl cyclase-interacting protein. *The Journal of biological chemistry* **279**, 46946-46953

41. Sato, M., Blumer, J. B., Simon, V., and Lanier, S. M. (2006) Accessory proteins for G proteins: partners in signaling. *Annual review of pharmacology and toxicology* **46**, 151-187

42. Blumer, J. B., and Lanier, S. M. (2014) Activators of G protein signaling exhibit broad functionality and define a distinct core signaling triad. *Molecular pharmacology* **85**, 388-396

43. Blumer, J. B., Smrcka, A. V., and Lanier, S. M. (2007) Mechanistic pathways and biological roles for receptor-independent activators of G-protein signaling. *Pharmacology & therapeutics* **113**, 488-506

44. Takesono, A., Cismowski, M. J., Ribas, C., Bernard, M., Chung, P., Hazard, S., 3rd, Duzic, E., and Lanier, S. M. (1999) Receptor-independent activators of heterotrimeric G-protein signaling pathways. *The Journal of biological chemistry* **274**, 33202-33205

45. De Vries, L., Fischer, T., Tronchere, H., Brothers, G. M., Strockbine, B., Siderovski, D. P., and Farquhar, M. G. (2000) Activator of G protein signaling 3 is a guanine dissociation inhibitor for Galpha i subunits. *Proceedings of the National Academy of Sciences of the United States of America* **97**, 14364-14369

46. Chauhan, S., Jelen, F., Sharina, I., and Martin, E. (2012) The G-protein regulator LGN modulates the activity of the NO receptor soluble guanylate cyclase. *The Biochemical journal* **446**, 445-453

47. Blumer, J. B., Lord, K., Saunders, T. L., Pacchioni, A., Black, C., Lazartigues, E., Varner, K. J., Gettys, T. W., and Lanier, S. M. (2008) Activator of G protein signaling 3 null mice: I. Unexpected alterations in metabolic and cardiovascular function. *Endocrinology* **149**, 3842-3849

48. Gao, J., Crapo, P., Nerem, R., and Wang, Y. (2008) Co-expression of elastin and collagen leads to highly compliant engineered blood vessels. *Journal of biomedical materials research. Part A* **85**, 1120-1128

49. Blumer, J. B., Chandler, L. J., and Lanier, S. M. (2002) Expression analysis and subcellular distribution of the two G-protein regulators AGS3 and LGN indicate distinct functionality. Localization of LGN to the midbody during cytokinesis. *The Journal of biological chemistry* **277**, 15897-15903

50. Friebe, A., Mergia, E., Dangel, O., Lange, A., and Koesling, D. (2007) Fatal gastrointestinal obstruction and hypertension in mice lacking nitric oxide-sensitive guanylyl cyclase. *Proceedings of the National Academy of Sciences of the United States of America* **104**, 7699-7704

51. Groneberg, D., Konig, P., Wirth, A., Offermanns, S., Koesling, D., and Friebe, A. (2010) Smooth muscle-specific deletion of nitric oxide-sensitive guanylyl cyclase is sufficient to induce hypertension in mice. *Circulation* **121**, 401-409

52. Nimmegeers, S., Sips, P., Buys, E., Brouckaert, P., and Van de Voorde, J. (2007) Functional role of the soluble guanylyl cyclase alpha(1) subunit in vascular smooth muscle relaxation. *Cardiovascular research* **76**, 149-159

53. Moro, M. A., Russel, R. J., Cellek, S., Lizasoain, I., Su, Y., Darley-Usmar, V. M., Radomski, M. W., and Moncada, S. (1996) cGMP mediates the vascular and platelet actions of nitric oxide: confirmation using an inhibitor of the soluble guanylyl cyclase. *Proceedings of the National Academy of Sciences of the United States of America* **93**, 1480-1485

54. Zanjani, K. S., and Niwa, K. (2013) Aortic dilatation and aortopathy in congenital heart diseases. *Journal of cardiology* **61**, 16-21

55. Kagota, S., Maruyama, K., Tada, Y., Fukushima, K., Umetani, K., Wakuda, H., and Shinozuka, K. (2013) Chronic oxidative-nitrosative stress impairs coronary vasodilation in metabolic syndrome model rats. *Microvascular research* **88**, 70-78

56. Abrams, J. (1996) Beneficial actions of nitrates in cardiovascular disease. *The American journal of cardiology* **77**, 31C-37C

57. Torfgard, K. E., and Ahlner, J. (1993) Effect of low dose of dipyridamole on glyceryl trinitrate tolerance in healthy volunteers. *Journal of cardiovascular pharmacology* **21**, 516-521

58. Surmeli, N. B., and Marletta, M. A. (2012) Insight into the rescue of oxidized soluble guanylate cyclase by the activator cinaciguat. *Chembiochem : a European journal of chemical biology* **13**, 977-981

59. Evgenov, O. V., Pacher, P., Schmidt, P. M., Hasko, G., Schmidt, H. H., and Stasch, J. P. (2006) NO-independent stimulators and activators of soluble guanylate cyclase: discovery and therapeutic potential. *Nature reviews. Drug discovery* **5**, 755-768

60. Zabel, U., Hausler, C., Weeger, M., and Schmidt, H. H. (1999) Homodimerization of soluble guanylyl cyclase subunits. Dimerization analysis using a glutathione s-transferase affinity tag. *The Journal of biological chemistry* **274**, 18149-18152

61. Bernard, M. L., Peterson, Y. K., Chung, P., Jourdan, J., and Lanier, S. M. (2001) Selective interaction of AGS3 with G-proteins and the influence of AGS3 on the activation state of G-proteins. *The Journal of biological chemistry* **276**, 1585-1593

62. D'Andrea, L. D., and Regan, L. (2003) TPR proteins: the versatile helix. *Trends in biochemical sciences* **28**, 655-662

63. Sans, N., Wang, P. Y., Du, Q., Petralia, R. S., Wang, Y. X., Nakka, S., Blumer, J. B., Macara, I. G., and Wenthold, R. J. (2005) mPins modulates PSD-95 and SAP102 trafficking and influences NMDA receptor surface expression. *Nature cell biology* **7**, 1179-1190

64. An, N., Blumer, J. B., Bernard, M. L., and Lanier, S. M. (2008) The PDZ and band 4.1 containing protein Frmpd1 regulates the subcellular location of activator of G-protein signaling 3 and its interaction with G-proteins. *The Journal of biological chemistry* **283**, 24718-24728

VITA:

George Britton was born in Houston, Texas on October 4, 1982 to Terttu L. Britton. He graduated from Langham Creek High School in Houston, Texas in May of 2002. After completing high school, George moved to Austin, Texas to study Neurobiology and Chemical Engineering at the University of Texas at Austin. After 5 years, he graduated, traveled, and settled back in Houston to work at the University of Texas Health Science Center as a research-assistant in the lab of Dr. Shao-Ling Huang. During this time, his research experiences directed him to undertake graduate level training in Biochemistry and Molecular Biology at UT-Houston GSBS. George's growing passion for research brought him to work for Dr. Emil Martin where he was able to gain a stronger foundation in his scientific knowledge and approach. He plans to continue his studies by undertaking a PhD program focused in Synthetic and Systems Bioengineering.